THE GEOLOGY, GEOCHEMISTRY AND ORIGIN OF SULPHIDE MINERALIZATION IN KATTA, WOLLEGA PROVINCE

A Thesis
Presented to
the Faculty of Science
Addis Ababa University

In Partial Fulfillment
of the Requirements for the Degree
Master of Science in Geology

by

Telahun Mammo

July 1980

ADDIS ABABA UNIVERSITY

School of Graduate Studies

The Geology, Geochemistry and Origin of Sulphide Mineralization in Katta, Wollega Province

by

Telahun Mamo

Faculty of Science

Approved by: _____

Prof. Roberto Valera _____
Advisor

Prof. J. Fabre _____
Examiner

Dr. R. F. Ball _____
Examiner

Ato Senbeto Chewaka _____
Examiner

Dr. Getaneh Assefa _____
Examiner

ABSTRACT

The Katta rocks form part of the Birbir group of the upper complex situated in the paleo-calc-alkaline arc that runs north-south across the country and which comprises thick sequences of metavolcanic and metasedimentary rocks. The rocks are intensely folded and faulted. Their mineralogy and texture indicate that metamorphism is of the greenschist facies.

Logging of five bore holes, their correlation and subsequent petrographic studies on selected samples are conducted and depth variation in mineralogy is presented.

Geochemical studies on stream sediments, bed rock and float samples, soil and core samples, and statistical treatment, of the results show that there is lateral and vertical variations in the copper and zinc mineralizations. The geochemical soil maps show that Cu, Zn, Pb, Ni, and Co mineralizations are concentrated along foliation and bedding planes. There is low lithological control of mineralization. Modal analysis on the core samples show that main mineralization is associated to carbonate.

Ore microscopic studies show that pyrite, chalcopyrite, magnetite, bornite, cubanite, bournonite, cuprite and sphalerite are the ore minerals found occuring in bands, as disseminations and in veins. Two types of mineralization are recognized syngenetic stratabound and epigenetic vein and disseminated types. It was the syngenetic type that gave rise to epigenetic types as a result of later metamorphic and supergene remobilization. The epigenetic type is considered to be the main mineralization in the area.

TABLE OF CONTENTS

	Pages
CERTIFICATE OF EXAMINATION	ii
ABSTRACT	iii
TABLE OF CONTENTS	iv
LIST OF FIGURES	vii
LIST OF TABLES	X
CHAPTER I INTRODUCTION	1
1.1. Purpose of Investigation	1
1.2 Location and Accessibility	1
1.3 Method of Approach	3
1.4 Acknowledgments	3
1.5 Previous Works	4
CHAPTER II GEOLOGY	6
2.1 REGIONAL	6
2.1.1 Previous Works	6
2.1.2 Stratigraphy	8
2.1.3 History	14
2.2 LOCAL	17
2.2.1 Introduction	17
2.2.2 Stratigraphy	18
2.2.3 Petrography	19
2.2.3.1 Surface Rocks	19
2.2.3.2 Subsurface Rocks	37
2.2.3.3 Summary & Conclusion	44

2.2.4 Chemical Analysis 45

2.2.4.1 Metasedimentary - Metavolcanic Sequence 45

2.2.4.2 Intrusives 48

2.2.5 Structure 48

2.2.6 Metamorphism 48

2.2.7 Alteration 53

2.2.8 Paleogeography 55

CHAPTER III ORE PROSPECTING 57

3.1 Introduction 57

3.2 Regional Geochemical Survey 57

3.3 Local Geochemical Survey 58

3.3.1 Stream Sediments 58

3.3.2 Bedrock & Float Samples 62

3.3.3 Soil Samples 75

3.3.4 Drilling 79

3.3.4.1 Introduction 80

3.3.5.2 Sampling System 81

3.3.4.3 Analysis & Data Presentation 82

3.3.4.4 Depth Variation 84

CHAPTER IV MINERALIZATION 89

4.1 Ore Petrography 89

4.1.1 Crushed Samples 89

4.1.2 Polished Sections 90

4.1.3 Summary & Conclusion 100

4.1.3.1 Mineralizing Events 110

4.2 Depth Relation 110

4.3 Stratigraphic (Lithologic) Relation 112

4.4 Lateral Relation (Variation) 114

4.5 Modal Abundance Relation 114

4.6 Tectonometamorphic Relation 115

4.7 Relation to Intrusives 118

4.8 Ore Genesis 118

4.8.1 Syngenetic Stratiform Mineralization 118

4.8.2 Epigenetic Vein - Disseminated Deposits 122

4.9 Other Copper Mineralization in Ethiopia 127

LIST OF FIGURES

Figure		Pages
1-4	General view of Katta	2
5	Geologic Map of Katta	Volume II
6	Mozambique and Phanerozoic Features	9
7	Major Tectono-Stratigraphic Units of the Ethiopian Precambrian	10
8	Plate Model for the Origin of the Ethiopian Precambrian	16
9	Stratigraphic Correlations of Drill Holes in Katta	Volume II
10	Microphotograph of Granite	31
11	Microphotograph of Calcareous-Chloritic Schist	31
12	Microphotograph of Quartz-Sericite-Phyllete	32
13	Microphotography of Quartz-Graphitic Phyllete	32
14	Microphotograph of Calcareous-Quartz-Sericite-Phyllete	33
15	Microphotograph of Silicified Quartzo-Feldspathic schist	33
16	Microphotograph of Microporphyritic Quartzo Feldspathic Schist	34
17	Microphotograph of Gneiss	34
18	Microphotograph of Metadiorite	35
19-21	Microphotographs of Core Samples	35-36
22	K_2O - Na_2O Graph for Metasedimentary Metavolcanic Sequence	46

23	K_2O - Na_2O Graph for Intrusives	48
25-26	Regional Geochemical Maps	59-60
27	Histogram of Total Copper for Stream Sediments	61
28-32	Histograms of Cu, Zn, Pb, Co & Ni for Bedrock Samples	63
33	Ternary Diagrams of Cu-Zn-Pb% for Core & Bedrock samples	66
34-39	Scatter Diagrams of the Elements for Bedrock Samples	70
40	High Copper-High Zinc Boundary	74
41-45	Histograms of Cu, Zn, Pb, Co & Ni, for Soil Samples	76
46-57	Geochemical Maps of Tulu Boli and Borokiss	Volume II
58-60	Geochemical Profile Sections of Tulu Boli, Enemay & Aderie Areas	Volume II
61	Sketch Showing Sites of Drill Holes	81
62-64	Scatter Diagrams for Elements of Drill Holes	83
65-69	Graphs Showing Highest Copper Assay Values against number of occurrences for drill holes	85
70-87	Ore Microphotographs of Representative Samples	101-109
88-89	Element content variation with depth	111
90	Depth variation in mineralogy	116
91	Superimposition of high Cu content on high Calcite content	117
92	Intrusion shown in regional scale	119

93	Superimposition of Katta's Pb-Zn% on Stanton's Pb-Zn% for world-wide marine volcanic sulphides	121
94	Idealized Profile showing relationship between intrusives, country rock and mineralization	125
CHAPTER V	CONCLUSION	131
	REFERENCES	133

LIST OF TABLES

Table		Page
1.	Correlation of Precambrian Stratigraphy of East Africa	7
2.	Stratigraphy of Mapped Area	19
3.	Stratigraphic variation in mineralogy	29-30
4.	Mineralogical variation with depth in DDH_4	38
5.	Mineralogical variation with depth in DDH_5	41
6.	Mineralogical variation with depth in DDH_7	43
7.	Na_2O - K_2O analysis for metasedimentary - metavolcanic sequence	45
8.	Silicate analysis for intrusives	47
9.	Variation of element with stratigraphy	64
10.	Cu-Zn-Ni values for ferruginuous outcrops & float samples	65
11-14.	Base metals assays for four localities	77-78

CHAPTER I

INTRODUCTION

1.1. Purpose of Investigation

Although a considerable amount of drilling and geochemical data are available for Katta little work was done on the geology, petrography and composition of the rocks. The mode of origin of the Cu - Zn - Pb - Ni sulphides has not been studied at all.

The purpose of this study is to provide new data on the geology and mineralization in the Katta area. Based on surface geological mapping on the scale of 1:12,500 of an area of about 35 sq. kms., geochemical mappings on the scale of 1:2500 of certain choosen localities and study of five drill holes within the locality of Katta 2, the stratigraphic relations of the rock units and distribution pattern of the elements are determined; Statistical treatment is done on the data to see the geochemical behaviour of the elements, and the relationship of the mineralization with the stratigraphy.

Based on the new data the origin and nature of the sulphide mineralization is discussed.

1.2. Location and Accessibility

Katta is located in Western Ethiopia about 10 kms. east of Nejo and is bounded by latitudes $9^{\circ}25'N$ and $9^{\circ}28'N$ and longitudes $35^{\circ}32'E$ and $35^{\circ}35'E$. The town of Nejo is 515 kms. from Addis Ababa, and is accessible by an all-weather road, which passes near the immediate southern margin of the area.

General View of Katta Fig. 1 - 4

As the area is highly dissected by rivers and streams with dense vegetation growing along their courses, accessibility is restricted along feeder roads that lead to the various mineral prospects within the area. It is only during the dry seasons from November to June that accessibility is possible by four wheel drive.

1.3. Method of Approach

Geological mapping is done by the author on the scale of 1:12,500 on an area of about 35 sq. kms. Map compilation of the adjacent area is also done to show the position of the drill holes. Petrographic studies are done on the outcrop samples and core samples to determine variation in composition and texture with depth. Ore petrography is carried out on representative polished sections to determine type, texture and structures of the ore minerals. Logging of the drill holes and correlation are done to establish vertical sequences upto a depth of about 225 m. Chemical analysis is done on more than 600 soil and rock samples collected and the results together with the data obtained from drill samples are statisticaly treated and subsequent discussion and conclusion are done.

1.4. ACKNOWLEDGEMENTS

The writer expresses his deep gratitude to Professor Roberto Valera for his valuable advices and for critically reading the thesis. Many thanks are also due to Ato Belay Desta, Dr. Getaneh Assefa, Ato Aberra Mogessie, Ato Senbeto Chewaka and staff members of the Geochemical Section in

E.I.G.S. for their advice and logistic support. Financial support from the Swedish Agency for Research Cooperation with the Developing countries (SAREC) obtained through the Ethiopian Science and Technology Commission, from the Addis Ababa University and from the Ethiopian Ministry of Mines, Power and Water Resources which was used to cover the expenses incurred in the research work undertaken and in the preparation of this dissertation is gratefully acknowledged.

1.5. Previous Works

Indications of gold mineralization in Katta were first discovered in 1880's, during which E. Combul prospected the region and formed "The Societe Anonyme des Mines d' or du Wollega," and obtained a large concession centred on Nejo.[1] Since then for about 90 years exploration works lay dormant. In the late 60's and early 70's works resumed by UN mineral survey and Cu - Zn - Ni geochemical anomalies were discovered. G.R. Kent (1970)[2] wrote the exploration results on the Katta primary gold occurrence followed by Kochemasov (1971)[3] who gave a summary of the geology and mineralization of the Metti - Nejo mineralized belt.

Subsequently, follow up works were carried out by the Ethiopian Institute of Geological surveys and The Metal Mining Agency of Japan (1974)[4]. In 1972 Geochemical soil samplings were done at four localities in Katta by Sisay[5] & Hailu[6]. The same year, geological mapping were done by Ahmad and Aklilu[7] followed by Faseka (1973)[8] and Aberra[9] (1973-74

who did the same work. Later on in 1977 Tesfaye[10], in 1978 de Wit et al[11] and in 1978 & 1979[12-13] Belay D. made mapping on the adjacent areas. J. Pisarski,[14-15] (1978) released two reports, one dealing with the geoch. assessment of western Wollega and the other a preliminary compilation of the geoch. works done in Katta. de Wit tried to briefly discuss control of mineralization in Katta and Belay logged one of the drill holes. Finally in 1980 two unpublished reports appeared: One by Kazmin et al [16] and the other by Ahmed [17]. Kazmin wrote about the metallogeny of western provinces and attempt to find a plate tectonics model for it. Ahmad wrote on the geochemical over burden exploration in Katta.

CHAPTER II

GEOLOGY

2.1. Regional

2.1.1. Previous Works

Since systematic geological exploration began only recently present knowledge of the precambrian in Ethiopia is poor. However the most common view includes the territory of Ethiopia in the Mozambique Belt-the structural zone stretching from Mozambique to Egypt and Sudan, and probably even to Saudi Arabia (see fig. 6). This Mozambique Belt was described by Holmes (1951)[18] as a late Precambrian geosyncline so deeply eroded that its inner highly metamorphosed parts are exposed on the surface. The same view was expressed by Cahen and Snelling (1966)[19], and later in 1970 by Clifford[20] who considers it as a "vestigeosyncline or mobile belt built up of remobilized ancient material."[11]

The Ethiopian Geological Survey and United Nation's Mineral Survey contributed much to the understanding of this belt in Ethiopia. Four areas of Precambrian rock outcrops are identified in Ethiopia (in Western, Eastern and Southern parts). For the northern area Dainelli's[21] (1943) and Beyth's (1972)[22] publications are available. For the eastern area Lebling and Nowack (1939)[23] gave a limited data of the basement. Glboy and Chatter (1960)[24] made a valuable contribution

Table 1. Correlation of some Precambrian unit in East Africa and Arabia

Age		Abs. Age	Saudia-Arabia	Egypt	Sudan	Ethiopia	Somalia	Kenya	Tanzania
Eocambrian		500 & 700	Fatima, Abla formations	Hammamat Series	Awat Series	Shiraro Fm. Matheos Fm.			
Upper Proterozoic	Upper part	1000	Murrdama Formation Halaban Formation	Schist-mud stone-grey-wake series Dokhan Series	Upper part Nafirdeib Series Lower part	Tambien Group Tsaliet group Birbir group	Inda-Ad Series		
	Lower part	1600	Beish, Lit	Shadli Series Barramia Rocks	Primitive System	Adola group Wadera group	Green-rock Series in the Basement System ?	Some green rock complexes in western Kenya (?) Embu & Ablun Series in central & eastern Kenya Turoka Series	Ukings, Konse, Ndembera Series Limestone-graphite Series
Middle ? Lower Protero-zoic		2500	?	?					
Archean			Ancient Gneiss	Orthogneis-ses of "Basement" Mitiq Series		Burji) Awata) Alghe) Konso) Gneiss	Gneisses of the Basement System	Basement System	Usagaran System

After Kazmin, 1972

to the Precambrian of the Gariboro area in southern Ethiopia. Mohr (1971)[25] made a compilation of all the available data upto his time. Later on Kazmin's works (1971, 1972a, 1972b, 1972c, 1975, 1976, 1978)[26-32] gave a better understanding of the stratigraphy and possible manner of evolution of the Ethiopian basement. Finally Senbeto and dewit[33] tried to fit the available data into the scheme of Plate tectonics.

2.1.2. Stratigraphy

The possible stratigraphy of the Ethiopian Precambrian units and their correlation to those of East Africa and Arabian are summarized in Table 1.

Paul Mohr[25] while making a compilation of all the available data upto his time, divided the metamorphic zones of the Ethiopian basement into epi-zone, meso-zone and cata-zone. Though these metamorphic zones have their origins in orogenesis which affected geosynclinal sediments, the significance and relationships of the zones, the original positions and orientation's of the sedimentary basins and the number of orogenesis involved cannot be accounted for.[25]

The other alternative is produced by dewit and Senbeto.[33] Based on the available data they attempted to classify the Ethiopian basement into four or five major tectonostratigraphic zones. (See figs. 6 & 7).

Zone 1. Calc-alkaline Volcanic Plutonic Belt.

This belt built on and into pre-existing continental crust represents ancient island arcs and can be traced for about 1,200 km. The belt is represented in the north (Tigre and Eritrea) by Tsaliet group. This belt consists of a volcano-sedimentary succession of metavolcanics of andesitic and dacitic composition, various volcanoclastic rocks, tuffs, rhyolitic agglomerates, phyllites, schists, quartzites and arkose with intercalations of cherts, marbles and ironstones, and diorite, granodiorite and granite intrusions. Strongly deformed bodies of early diorite and granodiorites (during event 3 - see under history) gave an age of upto 700 m.y. with K/Ar method[34] and even 800 m.y.[35] Intrusives produced during events 5 & 6 gave an age of 493 $\pm$ 10 and 556 $\pm$ 15 with K/Ar method in S.E. of Bombashi, Wollega; and granite intruding the younger meta-sediments of Birbir group in the Metti-Nejo belt gave an age of approx. 290 $\pm$ 10 m.y. with K/Ar method.[27]

Zone 1 traced southwards, in the Barro region, is involved in greater extent of deformation and greater amount of uplift with a pressure of 6 - 7 Kb and temperature of 650 - 750^{o}C[36]. Such pressure and temperature greatly affected the calc-alkaline rocks. For unknown reason the regional strike of the

rocks of this zone, from south to north, swings from north-west and then again to north-east. This belt is characterized by copper and/or copper-zinc and/or gold mineralizations, economic quantity being found in the north in Eritrea.

Zone 2. Western Ophiolite Zone

This belt runs through S.W. Ethiopia for some 500 kms. from the Kenya border to the Blue Nile and possibly further north. It consists of a metagabbro-serpentinized ultramafic complex, unconformably overlain by a sequence of probable deep water metasediments and ultramafic meta-volcano-clasties and metasilicic volcanics. This belt represents the lower part of the Birbir group.

Zone 3. Central High Grade Area

This zone is well observed just north east of Lake Rudolf and constitutes rocks consisting of a series of mafic gneisses and granulites layered biotite and hornblend gneiss, quartzo feldspathic gneisses and migmatited and paragneisses. It represents konso gneisses of the lower complex.

Zone 4. Eastern Metamorphic Belt

This belt consists of high grade gneisses and migmatites, and ophiloitic rocks. It represents Kazmin's lower, middle and upper (Adola & Mormora groups) complexes.

Zone 5. Southwestern Cataclastic Belt

This belt is a megashear along the Sudanese border and can be traced into a wide north-west striking intra-continental rift in the Sudan which is filled with upto 15 kms. thick phanerozoic continental sediments.

Kazmin et al [16] and Senbeto & de Wit[33] tried to fit the tectonostigraphic zones described above into the scheme of plate tectonics. But plate tectonics in the Precambrian is still a subject of considerable controversy and there are now basically two schools of thoughts: one argues that, according to the principle of uniformitarianism, global tectonics has evolved along essentially the same lines from the early Archaean to the Phanerozoic, and since plate tectonics is virtually an established fact in modern global evolution it must also have operated in the Precambrian.[37] The other school sees a fundamental difference in the tectonic evolution of most Precambrian mobile belts and Phanerozoic orogens and concludes that global tectonics may have evolved from an era of predominantly interaplate deformation to the present stage of predominantly plate margin tectonism.[38] Since the African continent contains a large number of Precambrian belts, it has featured strongly in this debate. Paul Mohr's attempt, as described earlier to make interpretation based on intraplate deformation left many problems unsolved.

Recently, however, de Wit and Senbeto grasping tightly the validity of plate tectonics concept to geology and orogenesis of the Appalachian and Caledonian Mt. belts which at least partly overlay in age with Pan African events, including those that gave rise to Mozambique Belt in Ethiopia, established a plate tectonics frame for the Ethiopian basement rocks. This is represented in figure 8. The teconics, history and associated events are explained by this model.

Zone 1, since it is built on and into pre-existing continental crust represents a paleo calcalkaline arc; zone 2 because of its characteristic rock association is designated to be a remnant interarc or back arc basin. Zone 3 is zone of high grade metamorphisic as a result of collision and subsequent subduction of oceanic crust below volcanic arcs, and hence represents an arc trench gap. Zone 4 which contains the A dola & Kenticha ophiolite belts represents intracontinental to intracontinental rifting. And finally zone 5 represents continent-continent-collision of African cration with an undefined eastern continent.

2.1.3. History

The following succession of events are constructed from available data and on the basis of de Wit and Senbeto hypothesis:

Event 1:

Formation of ancient Cratonic basement (Lower Complex) (2,500 m.y.)) and subsequent rifting.

Event 2:

Creation of oceanic lithosphere and accumulation of platform-type Psammitic and pelitic sediments to the Wadera Group (Middle Complex) and its equivalents in depressions on the ancient basement (1,000 m.y.).

Event 3:

Creation of oceanic lithosphere arrested and subduction westward beneath Sudanese Forland forming Pan African Andean type Continental Margin and Marginal Island arc system (900-750 m.y.)

Event 4:

Initiation of back are process which caused thinning and extension and eventual development of interarc basin (Adola, Mormora, and Lower Birbir Groups) (750 m.y.)

Event 5:

Continental Convergence accompanied by subduction caused are type volcanism and the deposition of Middle and Upper Birbir Group, Tsaliet and Tembien Groups (650 m.y.)

Event 6:

The high heat float accompanied the collision (arc-continent collision) led to the formation of

Himalayan-Tibetan type Mt. belt. This is indicated by the extensive development of alkali-granite ring complexes and associated extrusives over a wide zone.

2.2 Local

2.2.1. Introduction

The area forms part of the upper complex of the Wollega Birbir group consisting of metasedimentary and metavolcanic rocks. The Birbir group, which is correlated with the Tsaliet group of northern Ethiopia, the Halaban formation of south Arabia, the Dokan series of Egypt, and the lower part of Sudan, unconformably overlays older gneisses and amphibolites and related metadiorite - granodiorite intrusives.[27] The basement rocks probably outline a young irregular topogrphic paleo - landscape continuous volcanic and plutonic activity and the accompanied sedimentation is indicated by the presence of intermediate silicic metavolcanic (andisitic-dacitic-rhyolitic tuffs), lappli tuff, probably agglomerates and a vast amount of volcano-clastics, and by the presence of blue quartz porphyry.[11]

At least two episodes of deformations are recognized from field observations. The first one is characterized by the low grade regional metamorphism in green schist facies accompanied by the development of penetrative phyllitic and slaty cleavages,

large scale foldings and north-south trending faults. The second episode is characterized by the presence of small scale foldings crenulation cleavages and lineation and north-west and/or north-east trending faults. The general view of the area is shown in figures 1 to 4.

2.2.2. Stratigraphy

An attempt is made to establish a tentative vertical sequence based upon bore-holes drilled in neighbouring adjacent area upto a depth of 230 meters. The logging and subsequent correlation of the vertical sequences established for the five bore holes is presented in figure 9.

Petrographic studies show that there is a repetitive succession of different units upto the specified depth. The petrographic comparison between the different units encountered at depth and those outcroped in the mapped area seems to suggest that the two are generally identical mineralogically, though there is a variation in the contents (%) and type laterally as well as vertically. For borehole numbered DDH_4 mineralogical variation with depth is given in figure 90.

The repetitives sequence with depth may be due to the complicated structures represented by folding and faulting.

The stratigraphy derived from reconstruction based upon surface mapping is given below (Table 2).

Metasedimentary Rocks	Metavolcanic Rocks	Intrusives
	Calc. chlorite schist.	Granites
	Quartz sericite phyll.	
Quartz-graphitic phyll.		
Calc. quartz-ser. phyll.		
	Quartzo - feld. schist.	Gneiss
U N C O N F O R M I T Y		
		Metadiorite

(Table 2)

2.2.3. Petrography

2.2.3.1. **Surface Rocks**

Granite

The granites outcrop in restricted places. The contacts between these intrusives and the country rocks cannot be observed as they are buried beneath thick soil. However the contacts

with the accompanying hornfelsing are observed further west (Soukourokov, personal communication). Macroscopically the rocks are light coloured massive coarse grained with no visible sign of metamorphism. Microscopically the rocks show fractures along which chloritization of the feldspars is seen. Albite is by far abundant (0.5 - 1 mm. hypidiomorphic, rims or almost whole grain of ablite being replaced by microscophic quartz-albite intergrowth) due to later silicification or crystallization from eutectic point. Deformed twin lamellae are also observed. There is a tendency for albite to clustre together. The matrix is taken by interstitial, recrystallized (late) 0.1 mm biotite (green and brown) chlorite and muscovite. Recrystallized, xenomorphic quartz 0.1 mm, corroded and undulous are observed along with epidote. (See fig. 10).

Quartzo-feldpathic Schist

This is metavolcanic unit and covers large area. Macroscopically the rocks are compact, medium grained, gray to pink coloured and outcrop mainly in the western part of the area. They are highly sheared and silicified in places.

This unit can be subdivided into subunits based on

(i) intensity of deformation

(ii) silicification, and

(iii) texture

Silicified quartz-feldspathic Schist

This is intensely sheared and fractured, weakly schistose and fine grained subunit. Since the rocks are intensely silicified their identity is obliterated megascopically. Microscopic examinations, however, show that the rocks are very fine grained composed of two generations of quartz. The secondary quartzose bags containing albite intersect the schistosity planes thereby showing silicification is later than the development of schistosity. Crude incipient planes of bedding is seen and exhibits phyllite texture. The pulverized quartz is intimately associated with spangles of sericite mica and pyrite. The secondary quartz are angular with irregular outline. (See fig. 15).

Microporphyritic quartz-feldspathic schist

Microporphyroblasts of alkali feldspar and albite are observed set in the fine grained matrix of quartz, feldspar and sericite mica. The albite rims are altered to sericite. Crude schistosity is observed. (See fig. 16).

Quartz-sericite phyllite

This is a metavolcanic unit and covers large area. The colour of the rocks are generally greyish green. Quartz veins intrude this unit at various places. Macroscopic crenulation cleavages are observed.

Microscopically, the rocks are very fine grained with overall granoblastic - lepidoblastic texture and show effects of crushing. Fine spines of sericite mica exhibit microfolding of the schistosity planes and in saddles of folds very fine granulated quartz are observed. The rocks show shearing as observed from wisps of sericite flakes resulting probably in slip cleavage. Interspersed here and therein the quartzose materials are found granules of pyrite. The quartz grains show preferred growth parallel to the foliation. The shape of a crystal in a poly crystalline aggregates depends on the relative mobilities of the various parts of its boundary, thus, the orientation of micas in a quartz-micaschist may be the controlling influence on the dimensional orientation of quartz which will be elongate parallel to the micas.[39] (See fig. 12).

Quartz-graphitic phyllite

This unit occupies a very narrow zone that runs north south in the area. Macroscopically the rocks are dark, red even white in colour, compact and laminated in a millimeter scale.

This unit is further subdivided into three units based on

(i) colour

(ii) graphitic and pyritic content

(iii) recrystallization

Grey phyllite

The rocks are grey coloured and, in places, show sedimentary structures like cross bedding. Microscopically the texture is lepidoblastic and fine grained. Quartz and pyrite are predominantly found. Graphite content is very samll. The graphite content doesn't usually exceed 1% except in a few outcrops further to the west where it passes on to graphitic rock. Pyrite is a common associate of graphite and suggests the reaction between ferruginous silicates and volatile components of CO_2, H_2O, HCO_3^- etc. Well developed crenulation clevages are shown by the sericite mica around the pyrite cubes thereby showing the pyrites are pretectonically emplaced or syngenetic with the sedimentary unit. (See fig. 13).

Red Phyllite (ferruginous)

This subunit is always exposed on top of hills and passes on to grey phyllite in the valleys. The red colouration appears to be due to oxidized high iron content derived from weathered pyrite cubes. Microscopically the rocks are weakly schistose and show crenulation cleavage of the sericites. The sericites are highly coloured red. The texture varies from lepidoblastic to nematoblastic due to the presence of fibrous minerals.

Ferruginuous Quartzites

This subunit occurs as small discontinous lenses on top of hills along with the red phyllite. The rocks vary from pure white saccharoidal to brown ferruginous quartzite banded on milimeter scale. A varigated fragile and impure varity disintergrates into sandgrains under the blow of a hammer. The occurance, further to the west, of zone of martite-magnetite layers upto a metre in thickness and of association with sandstone bedding of about 1 meter[11] confidently make it of sedimentary origin. The different appearance of this subunit from the others may be due to structurally induced recrystallization. Quartz veins are also abundantly found. Microscopically

the rocks are medium/coarse grained with granoblastic xenomorphic texture compose of quartz grains in the main.

Calcareous Quartz-Sericite Phyllite

This is a metasedimentary conglomeratic unit and is exposed over large area. Megascopically and mesoscopically the rocks are medium to grey and puff. The presence of sericite flakes gives shiny lustre to the foliation surfaces. In places where the degree of deformation and metamorphism is very low, relict sedimentary structures, such as cross bedding, are seen.

The clasts are inequant varying from pancake shape or S-tectonites to cigar shape or L-tectonites with sizes ranging from ¼ x ¼ cm. to upto 30 x 20 or 25 cms. The cigar shaped clasts have their longest dimension in the north south direction following the strike and pointing out zone of maximum east-west stress. The clasts are predominantly phyllitic but dacitic-rhyolitic (quartz-plag-sericite) and quartzitic. To the north and west of the area the clasts become bigger and faulting and fracturing and the resulting brecciation are observed. Metamorphism seems to increase to the east in this unit as evidenced from segregation of dark (blotite) and light minerals (quartzo-feldspathic).

Based on microscopic studies the unit is further subdivided in two subunits. Their virtual relations have been determined on the basis of

(i) intensity of deformation, and

(ii) alteration

Lower Subunit

Megascopically, larger clasts are observed. Microscopically, however, intense shearing is seen resulting in the formation of kink folds of micas particularly sericite and a micro lineation is seen by the allignment of micas. Interspersed between micas is found highly pulverized quartzose material. The rocks exhibit a lepidoblastic texture with porphyroblastic calcite. (See fig. 14).

Upper Subunit

Megascopically smaller and finer clasts are observed. Microscopically it is a medium to fine grained, showing a slight elongation parallel to the banding. Along the schistosity planes are found knotes of bundles of porphyroblastic calcite.

Calcareous Chloritic Schist

This unit is exposed along north south trending fault and occupies a restricted place. Megascopically the rocks are coarse to medium grained, dark green, compact, massive to schistose. Microscopically they exhibit crude schistosity and lepidoblastic to granoblastic hypidio-xenomorphic texture. The porphyroblasts are calcite, amphibol and epidote with some albite and chlorite. The calcite is twinned and formed as a result of recrystallization. The mineralogical association suggest that these rocks are metamorphosed basic rocks. (Fig. 11)

Granite Gneiss

The unit occupies a restricted place along a river course and comprises of pale green banded rocks consisting of quartzo-feldspathic bands and lenses alternating with chlorite-amphibole rich bands and lenses on a millimeter-centimetre scale.

Since this unit defines the contact between the plutonic rocks and the overlying metasedimentary-metavolcanic succession, it probably represents zone of concentrated deformation (shear zone) due to ductility contrasts. The derivation of the rocks may be related to the mixing and grinding

of the mentioned rock units in slide zone, during which recrystallization and remobilization of elements played a major role.

Further to the west this unit flanks both sides of one of the elongated plutonic domes and reaches a maximum thickness of 200 metres.

Microscopically the rocks show gneissose texture with porphyroblasts of potassium feldspar surrounded by granular quartzo-feldspathic materials. (See fig. 17).

Metadiorite

This unit is the oldest and outcrops continuously in the adjacent western part of the area, as along the Dilla river. It occupies the hinge zone of the major anticlines. Megascopically and microscopically ore minerals as magnetite and pyrite and in lesser amount chalcopyrite and malachite stains are observed. Microscopically, the rocks are medium grained with hypidioxenomorphic texture and contains amphibol epidote and chlorite. The hornblend are approx. 0.5 mm in size. The plagioclase shows saussoritization. (See fig. 18).

The stratigraphic variation in mineralogy (%) is summarized and tabulated below. (Table 3)

Unit	Subunit	Porphyroblasts/ phenocrysts (%)	Matrix (%)
Granite	-	Quartz (30) Albite (70)	Biotite (22) Chlorite (10) Muscovite (5) Epidote (3) Quartz)) 60 feldspar)
Quartzo-felds-pathic schist	(a) Silici-fied	Quartz (40) Albite (25) Sericite (7) Muscovite (3) Opaque (25)	Quartz) 100 feldspar)
	(b) Porphyro-blastic	Alkalifeldspar (40) (Orthoclase) Altered plagio-clase (40) Sericite (20)	Qurtz* felds-par (90) Sericite (10)
Quartz-Sericite phyllite	-	-	Quartz (60) Sericite (40) Opaque (1)
Quartz-graphitic Phyllite	(a) Grey Phllite	Opaque (100)	Quartz + felds-par (70) Opaque (20) Sericite (10)

	(b) Red phyllite	-	Sericite (50) Quartz (30) Opaque (15) Muscovite (5)
	(c) Quartzite	Quartz (100)	-
Calcareous quartz Sericite phyllite	(a) Upper	Calcite (100)	Calcite (20) Quartz+feld (45) Sericite (33) Muscovite (2) Opaque (5)
	(b) Lower	Calcite (90) Quartz (5) Muscovite (20)	Calcite (25) Sericite (40) Quartz+feld (30) Opaque (2) Muscovite (3)
Calcareous-chlorite schist	-	Calcite (30) Chlorite (40) Amphibol (15) Epidote (10) Plagioclase (5)	Plagioclase (20) Chlorite (20) Amphibol (25) Muscovite (30)
Gneiss		Quartz (Feldspar (40)	Sericite (40) Quartz+feld. (60)
Metadio-rite		Actiono-lite (50) Blotite (15) Plagioclase (35)	Epidote (30) Quartz (5) Chlorite (50) Sphene (5) Carbonate (10)

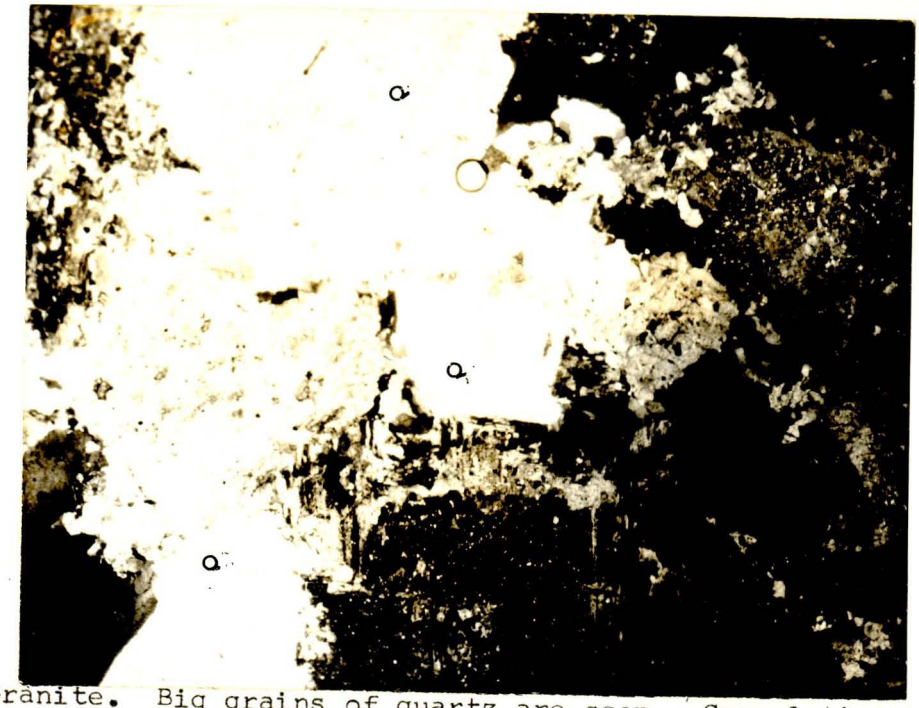

Granite. Big grains of quartz are seen. Granulation between the quartz grains suggest that the rock has undergone metamorphism. Parallel Nicols. Magnification 60 X
Fig. 10.

Calcareous Chloritic schist. Secondary Calcite (C) crystals are seen arranged parallely along foliation direction. Epidote (EP) is scattered throughout. Amphoboles (AM) have parallel orientation with the schistosity. Parallel Nicols. Magnification 60 X
Fig. 11.

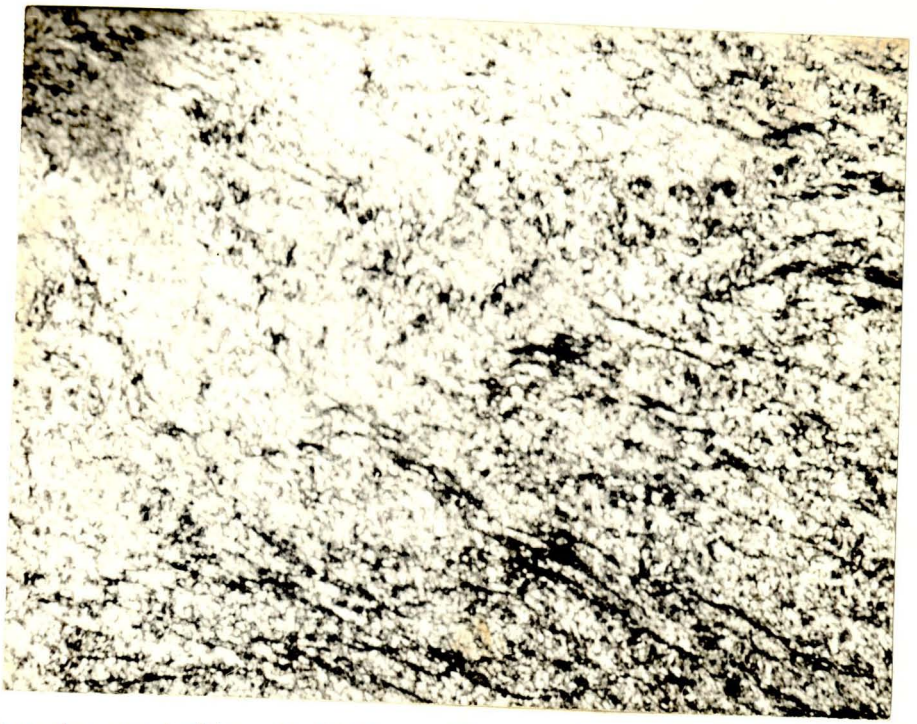

Quartz-sericite phyllite. Fine spines of Sericite mica exhibiting microfolding of the schistosity plane.
Fig. 12.

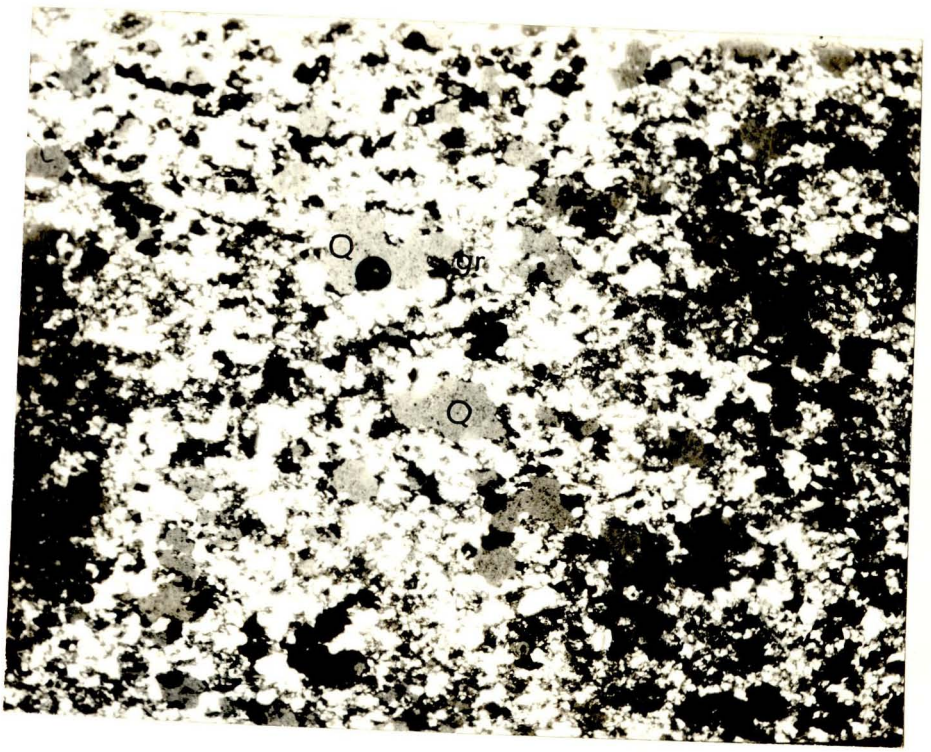

Quartz-graphytic-phyllite. Quartz grains (Q) are seen, the smaller white patches in the background are quartz and feldspar and Opaque minerals. Graphite (GR) is seen as dark dusty appearance. Parallel Nicols. Magnification 60 X
Fig. 13.

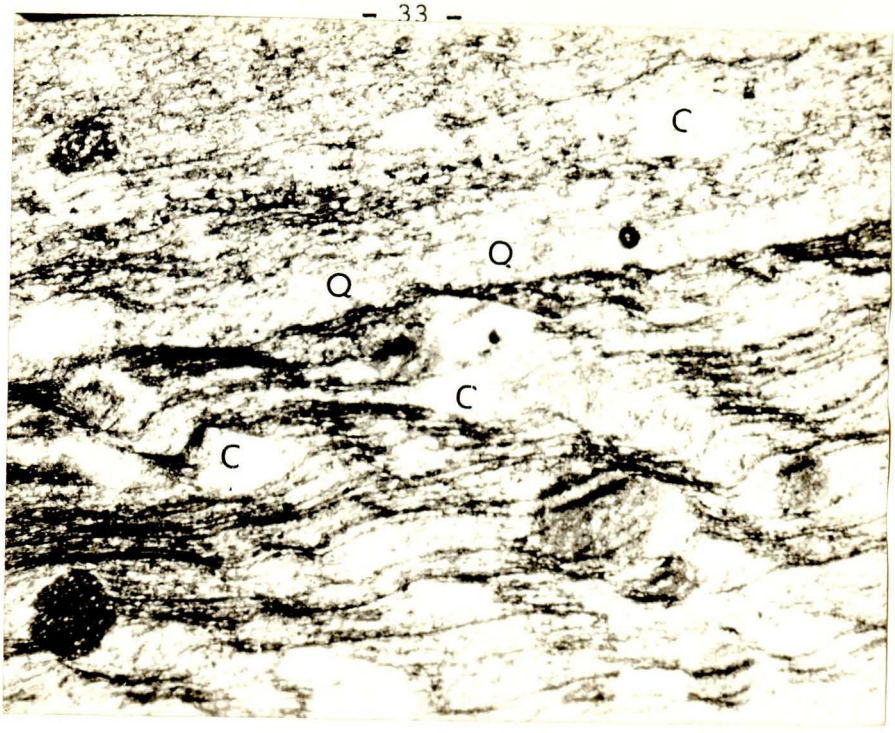

Calcareous quartz-ser. phyllite. Bundles of Calcite (C) entangles within Sericite (S) cords. Crenulation cleavage is well developed. Parallel Nicols. Magnification 60 X
Fig. 14.

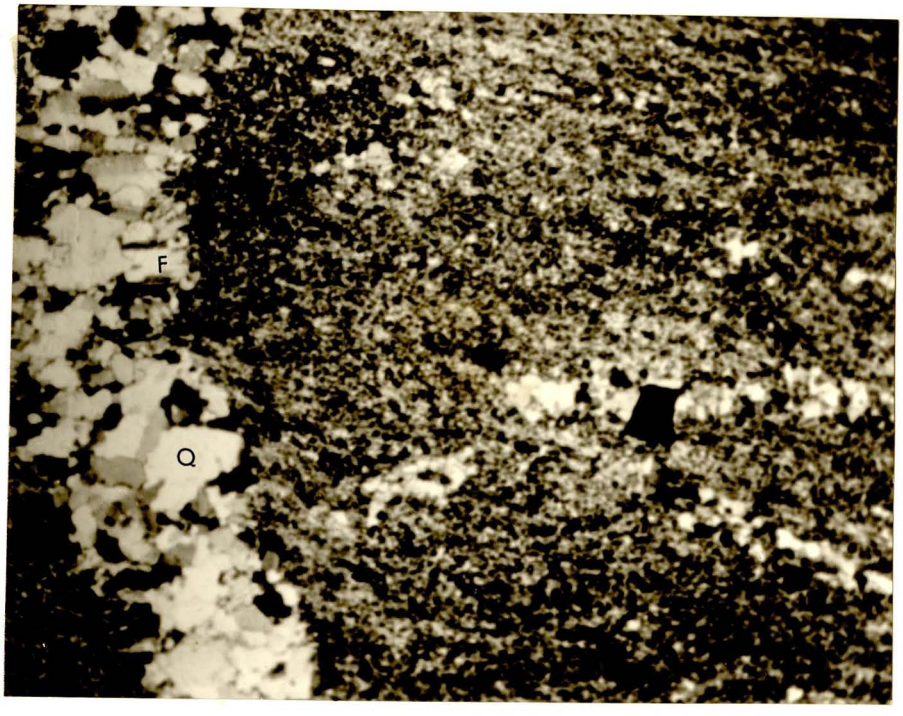

Silicified quartzo feldspathic schist. Secondary quartz-feldspar vein cross-cutting the Schistosity planes. The feldspars are mainly albite. Q = quartz and F = feldspar. Parallel Nicols. Magnification 60 X
Fig. 15.

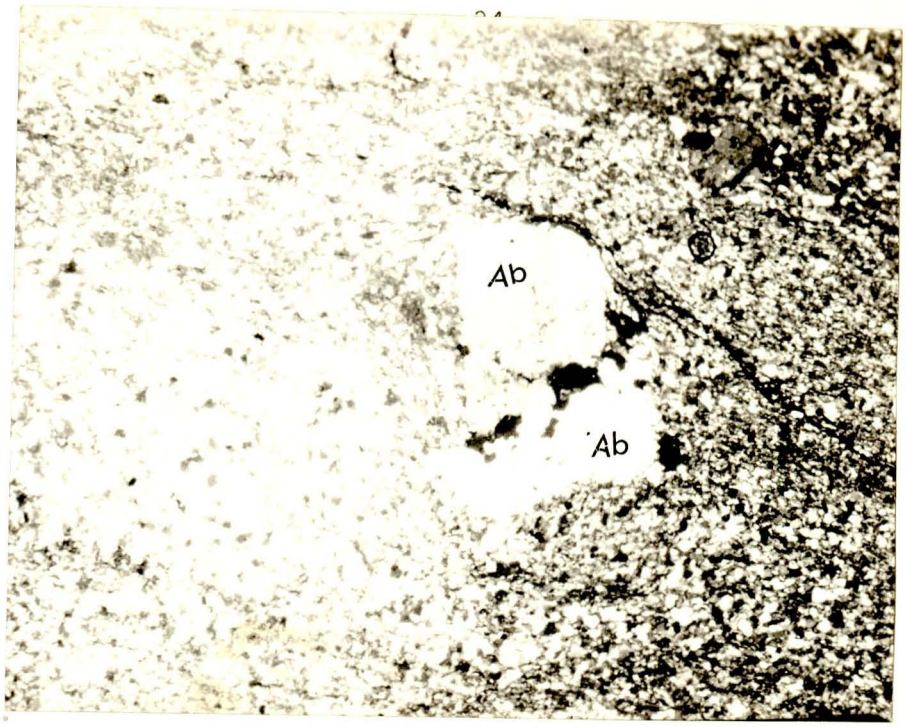

Micro-Porphyritic quartzo-feldspathic schist. Albite is seen clustered in the fine matrix composed of quartz, feldspar and Opaque minerals. Sericite is seen making bands about the albite (Ab). Parallel Nicols. Magnification 60 X.
Fig. 16.

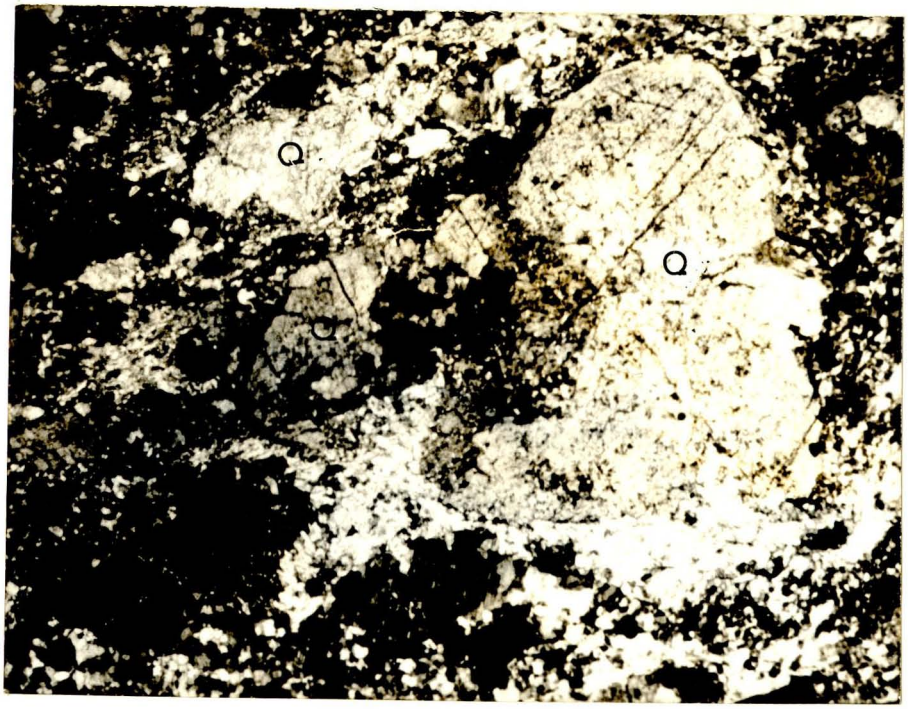

Gneiss. Granulated and fractured quartz are seen. In between bigger grains, granulated and crushed finely grained quartz and feldspars are seen. Parallel Nicols. Magnification 60 X
Fig. 17.

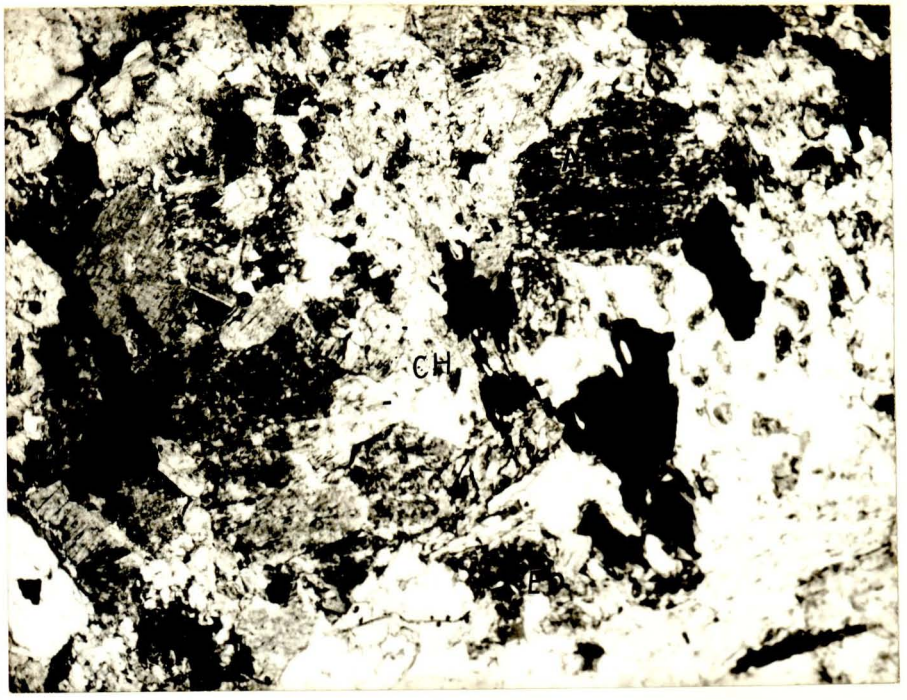

Metadiorite. Medium grained, with hydro-xenomorphic texture containing amphibol (AM), epidote (EP) and chlorite (CH). Parallel Nicols. Magnification 60 X
Fig. 18.

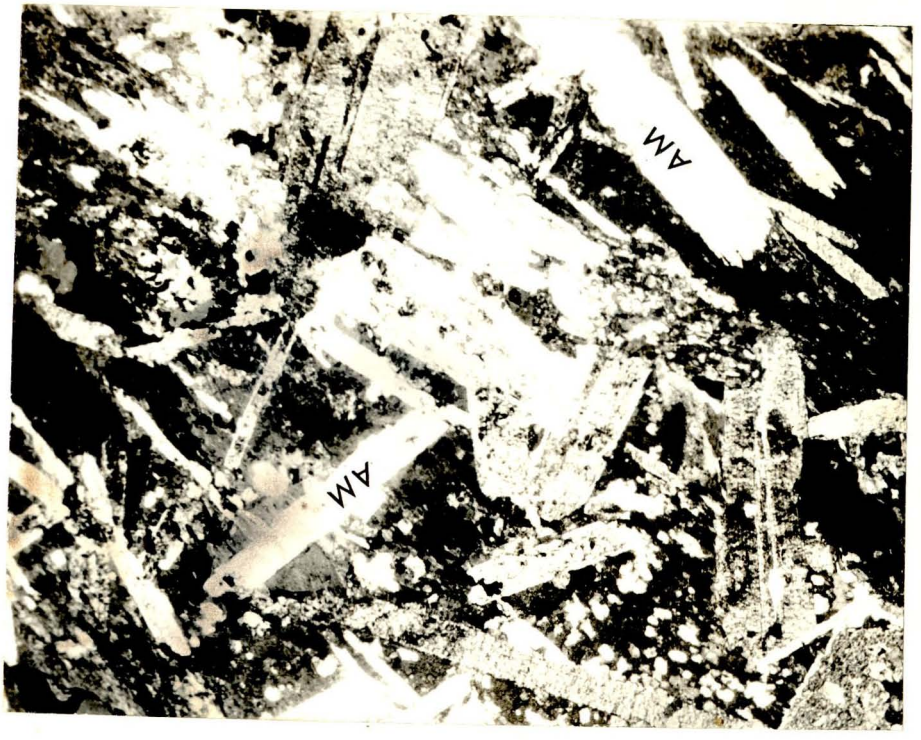

Core samples (DDH_4) at 180 m. depth. Very big crystals of amphibole (AM) set in fine matrix consisting of feldspars and amphiboles. Parallel Nicols. Magnification 60 X.
Fig. 19.

Core samples (DDH_4) at 70 m. depth. Calcite (C) porphyroblasts set in fine matrix consisting of calcite, feldspar & amphboles. Parallel Nicols. Magnification 60 X.
Fig. 20.

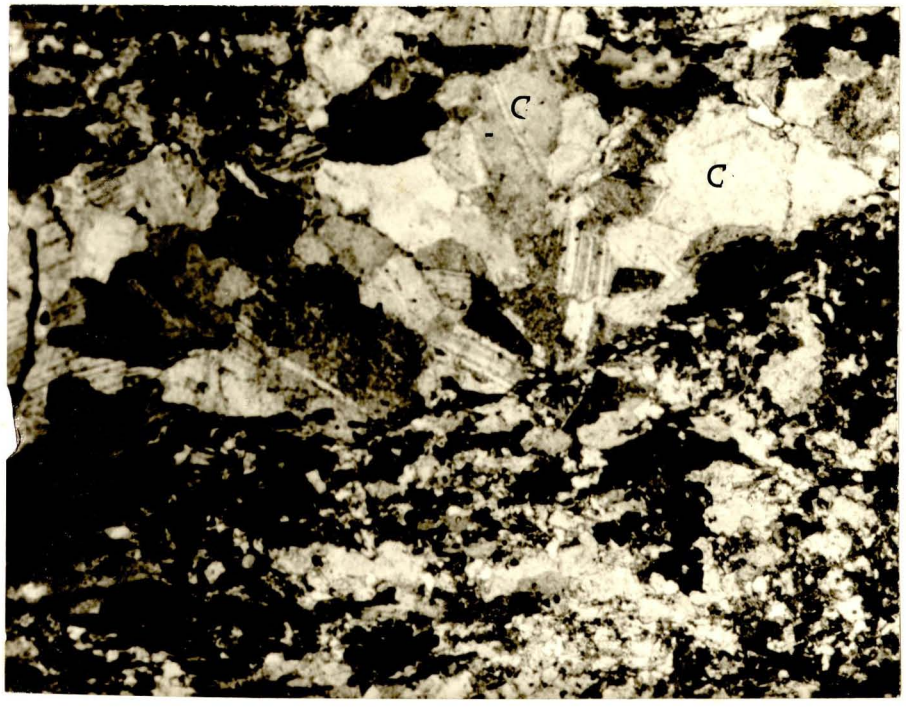

Core samples (DDH_4) at 90 m. depth. Carbonate vein cutting the rock. Parallel Nicols. Magnification 60 X.
Fig. 21.

2.2.3.2. Subsurface Rocks

DDH_4

Macroscopic Study

The maximum depth reached is 150 metres. The core samples examination seems to suggest a somewhat similar lithology throughout with intrusive bodies encountered every now and then. Upto a depth of 115 metres chloritic schists of differing composition persist. The schists are highly weathered towards the top of the stratigraphic succession, poorly foliated and the colour varying from purple to green. Crenulation cleavage are observed at depth. The diorite encountered at 48 m. depth is dark green compact with white siliceous upper contact and shows dendritic structure formed by the flow of manganese rich fluid. At 70 m. depth deep green chloritic schists often with mineral segregation, numerous quartz-carbonate veins, crenulation cleavage, with deep of foliation almost vertical (i.e. 45° to core length) are seen. Further down, in the same unit dip of foliation seems to vary between 30° and 40° to core length; kink bands, microfolds and crenulation cleavage are also observed. At 115 m. depth white medium grained siliceous marble with minor patches of dark green chlorite schists

is met. Lastly at depth of 131 m. is seen deep green mottled basic schists (amphibolite) which is weakly calcareous in general highly calcareous locally at top, middle and base of the central portion. Quartz-carbonate veins are observed in this unit.

Microscopic Study

Microscopic study is done on about 50 thin sections. The mineralogical associations and their variation with depth of selected samples are given below: (Table 4)

Metre (Depth)	Mineralogical Association
34.8	Biotite-amphibole-feldspar-opaque mineral
56.7	Amphibole-feldspar-opaque mineral
57.6	Amphibole-feldspar-opaque mineral
72.4	Calcite-amphibole-feldspar
104.7	Quartz - epidote - feldspar
105.3	Epidote - quartz, feldspar
106.4	Epidote - (Biotite)
106.8	Chlorite - quartz - plagioclase
111.1	Calcite - Epidote - Chlorite
111.9	Calcite - quartz - epidote - chlorite
112	Quartz-epidote-chlorite-amphibole
112.6	Epidote-chlorite-biotite-opaque
112.8	Quartz - calcite

130.4 Calcite-quartz-feldspar-epidote chlorite

140.5 Epidote-chlorite-amphibole-feldspar-opaque mineral

From the microscopic study it is concluded that epidote, chlorite and calcite, feldspars and in some cases amphibole occupy by far the greater percentage by volume of the constituents (see model abundance). The overall texture varies from lepidoblastic to porphyroblastic and the structure from schistose to massive depending on the degree of metamorphism and extent of recrystallization. The shape of the individual grain is mainly hypidiomorphic. Secondary twinned calcite are observed in many of the thin sections as porphyroblasts or in some cases as veinlets. Representative thin sections are presented in Fis. 22-24. There is a general increase with depth in epidote, calcite and amphiboles though biotite appear suddenly at depth to be cut off soon and disappear. Sercite however is limited to shallow depths.

Deformation and intensity of schistosity increases downwards and polyphase deformation can also be recognized. However, below depth of 131 meter decrease of deformation is observed.

DDH$_5$

Macroscopic Study

Macroscopically there is no significant variation with lithology upto a depth of 95.4 metres apart from the dioritic body encountered every now and then. Alternating purple to light green finely laminated and weathered talc chlorite and chlorite schists sometimes with manganese traces forming dendritic structure is seen at 28.3 m. depth. In places these rocks are micro-folded with dip of foliation ranging between 50° and 60° to core length at 48.8 m. depth. At depth of 95.4 m is seen compact undifferentiated green-schists (mainly chlorite schist and amphibolite) with variable carbonate content; well developed schistosity dipping 45° to core length and micro-foldings. Again at 109.6 m. depth deep green mottled amphibolite is met with alterate quartz - carbonate in the lower portion at 45° to core length, variable carbonate content; foliation often poor or nondeveloped.

Microscopic Study

Microscopically the rocks show massive to schistose structure. In some thin section a tendency for the epidote to clustre together is seen. The texture is generally granular. The depth variation in mineral association is presented below. (Table 5).

Depth (m)	Mineral Association
17.6 - 25.1	Sericite - chlorite - albite
31.6	Sericite-chlorite-graphite-quartz
36.9	Sericite-chlorite-albite
41.3 - 45.6	Albite-epidote-mica-chlorite
45.6-49.9	Muscovite-biotite chlorite-epidote
49.9 - 55.2	Muscovite-chlorite-epidote-albite
58.5	Quartz-albite-epidote-chlorite
65.5 - 76.7	Albite-chlorite-epidote-sericite
76.7	Sericite-Muscovite-chlorite-pyrite - chalcopyrite
92.8 - 98.2	Chlorite-Muscovite-albite-pyrite
102.5	Epidote-chlorite-pyrite-chalcopyrite
108.95	Epidote-chlorite-calcite-pyrite - chalcopyrite

Sericite seems to be a ubiquitous mineral and suggest that alteration is prominent in the rocks. Otherwise epidote chlorite and albite are the abundant minerals found in most thin sections.

DDH$_6$

Macroscopic Study

Towards the top of the bore hole, the rock types are weakly purple to deep purple chlorite schists, and bright brown to light green finely laminated phyllite with sericite-rich lighter

coloured layer (1-2 mm). Both the schists and phyllites, in places, contain fine to coarse, rounded to angular, siliceous to intermediate derived clasts, with some interlaminated grey graphitic looking, polyphase deformed schists at at 51 m. With depth increase of volcanoclasts and decrease of deformation are observed. At 55 m. depth poorly foliated while weathered sericite chlorite, schist, with contact appearing to dip opposite to foliation at 40° to 35° is seen. At 92.6 m. depth is seen deep green (mottled) calcareous undifferentiated phyllite and amphibolite, qz-carbonate differentiated at the top making alternate planes with the schist. Dip of quartz-carbonate and foliation of schist 40° to 45° to core length.

Microscopic Study

Microscopically some representative samples are studied. The studied samples show over all fine grained texture with no clear structures and/or deformations.

DDH$_7$

Macroscopic Study

The bore passed through a variety of phyllites, schists and intrusive bodies. Macroscopic observations show the upper part, upto 70 m

depth, to contain intercalations of pale grey conglomeratic phyllites and greenish grey volcanoclastics, with minor sericite schists and graphitic phyllites. This is followed by a 102-metre section of dark grey and green laminated phyllites, green becoming predominant at depth. The last 50 metres is made-up of uniformly green clastic schists and phyllites associated with swarms of quartz veins. The clasts are pinkish, and are uniformly distributed throughout the rock.

Microscopic Study

Microscopic study of samples taken at different depths reveal the following mineral association: (Table 6).

Depth (m)	Mineral Association
30	Calcite - quartz - feldspar
59	Calcite - quartz - feldspar- - chlorite - ore mineral
174	Quartz - minor calcite
201.5	Epidote - chlorite - quartz - feldspar - ore mineral
206.4	Plagioclase-chlorite-muscovite - calcite-quartz-epidote
210.0	Plagioclase-epidote-chlorite-calcite
219.2	Plagioclase-chlorite muscovite-epidote-quartz
224.8	Plagioclase - chlorite - quartz - calcite

Samples taken at 206.4 and 219.2 metres depth showed thatthe rocks essentially contain oligoclase, chlorite and muscovite with subordinate carbonates and accessory quartz, epidote, sphene and opaque minerals. The oligoclase is partly sericitized. The rocks show lepidoblastic texture, often with crenulation cleavage. Sample taken at 224.8 m. showed the rock to contain plagioclase, chlorite, quartz with subordinate calcite, and opaque minerals. The plagioclase, albite-oligoclase, is strongly sericitized. The rock is of granular texture, sample at 30 m. depth show qpartz carbonate vein. The carbonate (calcite) shows twinning.

The well defined crenulation lineation together with the large scale folding and the well developed axial planar cleavage, show the rocks to have undergone at least two periods of intense deformation.

2.2.3.3. Summary and Conclusion

Petrographic studies done on DDH_4, DDH_5, DDH_6 and DDH_7 made the following conclusions possible:

a. Generally greenschists are the result of differential alteration of a granodiorite/diorite intrusive stock. Exceptions are those derived from amphibolites.

b. Vertical variation in the type and content of the constituent minerals is observed.

- Calcite, ore minerals and amphiboles show an increase with depth.
- Biotite is restricted in occurrence
- Quartz, feldspar, epidote, chlorite persist with varying amounts throughout.
- Sericite appears only at shallow depths

c. Lateral variation in mineralogy metamorphism, and structure is observed.

- Southward decrease in carbonate observed i.e. from DDH_4 to DDH_7 . This is also supported by important conclusion given under "modal abundance".
- Southward decrease in metamorphism, (deduced from mineralogical association) and deformation intensity.

2.2.4. Chemical Analysis

2.2.4.1. A. Metasedimentary - metavolcanic sequence

For eight representative rock samples Na_2O and K_2O contents are analysed and the following results are obtained: (Table 7).

Samples	Na_2O	K_2O
1320	1.4	2.8
1326	3.8	8.6
1323	1.2	1.9
1321	2.0	1.8

T_{15}	0.6	3.3
T_{44}	4.2	4.5
T_{52}	3.4	1.7
T_{0}	0.1	0.1

Graph for K_2O against Na_2O content is constructed (see fig. 22). A higher K_2O content than Na_2O content is seen in general.

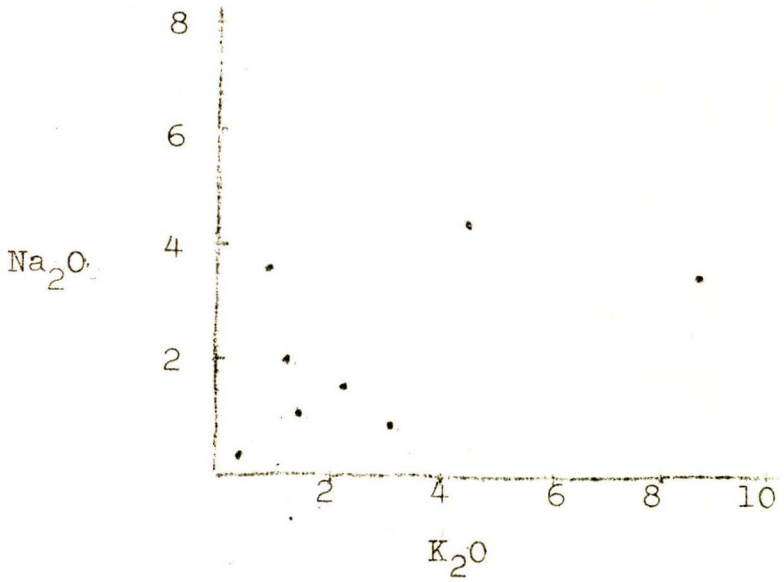

Sample Number	SiO_2	Al_2O_3	Fe_2O_3 (total)	TiO_2	MnO	CaO	MgO	Na_2O	K_2O	Moist -110°C	L.O.I. above 110°C	Sum
148010	68.8	13.9	4.9	0.4	0.1	1.0	0.7	4.9	3.1	0.1	1.3	99.1
148019	70.5	14.5	5.2	0.2	0.4	0.3	0.8	4.3	2.5	0.1	1.7	99.7
148029	45.5	12.3	18.3	3.0	0.2	9.4	5.9	2.8	0.4	0.1	1.4	99.2
148030	48.1	13.4	17.6	3.0	0.2	6.3	5.2	4.0	0.2	0.1	2.1	100.2
148040	63.5	16.9	3.2	0.5	0.1	0.9	3.9	8.1	0.2	0.3	2.3	99.8
148043	52.5	13.8	13.6	3.0	0.3	5.3	3.7	4.9	0.3	0.1	1.6	99.1
148045	51.7	11.1	10.2	0.5	0.1	7.7	5.3	3.5	0.3	0.1	9.3	99.8
148074	49.5	14.9	12.4	1.6	2.2	8.3	5.9	3.7	0.1	0.7	2.4	99.7
149068	61.6	16.7	7.1	0.8	0.1	0.6	4.3	4.2	1.5	0.3	3.1	100.2
149073	57.5	16.9	9.0	0.8	0.1	0.5	4.3	5.0	1.6	0.8	3.5	100.0
149092	58.2	17.5	6.8	0.6	0.1	1.3	5.0	7.3	0.4	0.1	2.8	100.0
149105	70.4	13.3	5.7	0.4	0.1	1.5	0.9	5.5	0.8	0.1	1.0	99.6

(Table 8)

(After- Soukourokov, unpublished)

Results are in percentage

2.2.4.2. B. Intrusives

Most of the intrusive rocks as deduced from petrographic studies and silicate analysis are of quartz dioritic composition (see Table 8). The K_2O percent distribution is plotted against Na_2O percent distribution (fig. 23). The result shows higher Na_2O content.

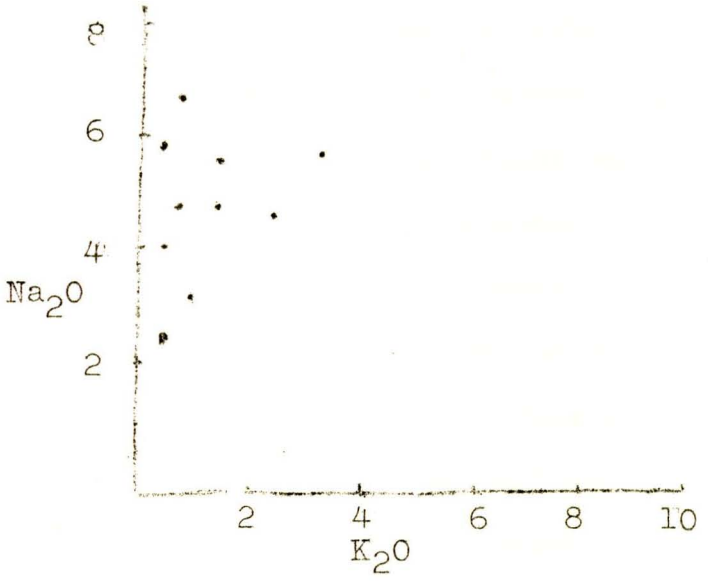

2.2.5. Structure

Because of lack of exposure and structural complication of the area no accurate structural interpretation is possible. However, some attempt is made to unravel the structural features including the number of deformation episodes affected the area. At least two deformation episodes are identified.

First Deformation (D_1)

This period of deformation has been inferred from the presence of intense penetrative deformation in the rocks resulting in the development of large scale folding (A_1) associated with a well developed axial planar schistosity (S_1) which often completely transposes the original sedimentary layering (So). The east-west d direction of the deformative force (F_1) resulted in the formation of submeridional or north south trending major faults of the area. The predominantly NNE-SSW penetrative schistosity was developed because of the intense flattening the rocks underwent. Series of synforms and antiforms are recognized plunging on the average 9° SW in the eastern half and about 7° NE on the average in the western half. This is inferred from the plunging of lineations (L_1) as they reflect the attitutde of megastructures (folds). The axial plane and the associated schistosity are sometimes vertical but generally dip to the west at an angle of about 70° on the average. Diamond drilled core samples suggest an even steeper dip and possibly an overturning to the east. Recognition of folds was a challenge to the field work but was resolved using conventional structural field techniques such as facing and bedding/cleavage relationships.

The amplitude of these folds was determined in adjacent area and varies between 100 and 200 meters with a wave length variation between 200 and 600 metres.

The clasts in the conglomeratic sequence are deformed differently at different places. They generally vary from S-tectonite to L-tectonite, hence mode of deformation varies from a flattening to a constrictional type. On the south of the mapped area the L-tectonites are well developed whereas in the central and on northern portion the S-tectonites predominate. The L-tectonites conform with the foliation plane. The difference in the strike of foliation direction and strike of bedding ranges from 5^{o} to 20^{o}.

Second Deformation (D_2)

This deformative force (F_2) was less in magnitude as its effect is not of regional importance. This however led Belay[12] to conclude that this D_2 was actually part of D_1 as its effect is seen only in incompetent beds. Tesfaye[10], however sees it differently and says that there are two kinds of microfolds, (as D_2 is best manifested by small scale folds of 1 to 20 metres amplitude with crenulation cleavages that vary from well developed to poorly developed) one that affected the S_1, the other that did not affect S_1 and concludes that the two are different in ages and hence belong to different deformation

stages. However field observation seems to support Tesfaye's view.

The folds are gentle with sublatitudinal and NW-SE trends superimposed on the first phase folds (A_1). At certain localities in A_2 folds vertical lineations (L_2) are observed with vertical axial planar schistosity (S_2). Throughout the area, however, refolding of the first cleavage and development of crenulation cleavage is observed. Evidence for second deformation is the formation of steep secondary cleavages in the same direction. These secondary cleavages produced crenulations in already foliated sediments.

This deformation episode is characterized by two kinds of faults having sublatitudinal (Aden Gulf direction). In some of these faults brecceation and mylonitization are observed. This is well seen in the northern and western parts of the area.

Conclusion

The study suggests that the initiation and development of the first and main deformation episode was the result of continued compression following continent-arc collision that was marked by the colosure of interarc basin.

Immediately after or during compression of the first period acting east-west, a greater amount of uplift with pressure of 6-7 kb. and a temperature of

650-750° in the Baro region[36] took place. Becuase of this compression and the uplift a lifting of the megastructures axes might have taken place thereby constituting the second deformation.

2.2.6 Metamorphism

Typical mineral assemblages found at Katta metamorphic sequences are:

Quartz-sericite

Quartz-calcite-sericite

Quartz-albite-sericite

Orthoclase-quartz-sericite

Calcite-chlorite-actinolite-epidote

Actionolite-epidote-chlorite

Actinolite-epidote-calcite

Epidote-chlorite-muscovite

Muscovite-actionolite-quartz

Biotite-muscovite-chlorite-quartz

The rocks underwent regional metamorphism in the greenschist facies during first deformation episode. The metamorphism grade seems to increase to the east as observed in the Tulu Boli are where the rocks are mostly biotite schists. Segregation of minerals in thin bands are also seen southwards.

The second deformation episode is seen in recrystallization. Around the intrusive bodies no sign of contact metamorphic effect could be seen

because of lack of exposure or have been obliterated by hydrothermal alterations.

Since the rocks of this facies are formed at lowest metamorphic temperatures, they are characterized by hydrous minerals and absence of garnets and pyroxenes of higher facies. However, there are actinolite amphiboles resulting from the conversion of aluminous hornblend of higher facies as chlorite become increasingly abundant[40]. Generally two subfacies are recognized in this facies: higher grade biotite-chlorite subfacies and lower grade muscovite-chlorite subfacies. where the metamorphic grade increases especially to the east, biotite - chlorite subfacies are found. At lower metammorphic grade which is dominant in the region, muscovite-chlorite subfacies are observed.

2.2.7. Alteration

Because of the complexity of the structures, it is difficult to delineate the different zones of alternation accurately. Nevertheless the different alteration zones are given below.

(1) Chlorite-epidote-calcite alteration zone.

This is found at depth and shows complete replacement of amphibole and biotite by chlorite and epidote. Minor amount of feldspar is also replaced by epidote and calcite. Chlorite could also be

formed as a result of replacing acidic glass in tuff and lavas.[41] This therefore suggest that the overall intensity of alteration is weak to moderate. In this zone ore mineralization i.e. pyrite and chalcopyrite content are maximum.

(2) Sericite - alteration zone

This is found at a very shallow depth. Complete replacement of plagioclase to sericite has taken place. Minor amounts of quartz, chlorite and pyrite are observed. The sericite could also be formed by replacing acidic glass in tuff and lavas.

(3) Biotite - alteration zone

This is in between the above two zones. The amphibol of the volcanics and volcanoclastics have been altered to green biotite. Some chlorite and epidote are associated. This zone passes onto chlorite - epidote - calcite zone. Pyrite is also found.

(4) Silicification

Silicification occurs along highly sheared zones. Microscopic examination reveals a mosaic of coarse grained quartz with subordinate amount of slbite, sericite and muscovite. This may be gradational to sericite or chlorite - epidote - calcite alteration zones.

Conclusion

The alteration could have been brought about by both

(i) hydrothermal solutions and

(ii) regional metamorphism

However, the effects of the two cannot be distinguished.

2.2.8. Paleogeography

The area forms part of the Birbir group of the upper complex. The manner of deposition of the Birbir group is discussed here.

After the formation of cratonic basement 2,500 m.y. ago, due to upsurging of mantle plumes, doming, fracturing and subsequent rifting with ultimate oceanic lithosphere formation took place. Creation of oceanic lithosphere stopped at certain stage, may be due to change in the geography of the convective current. Westward subduction was initiated forming Andean type continental margin. Later on interarc basin was created due to thinning and extension of the arc itself. Deposition of lower Birbir group took place in the basin 750 m.y. ago. The closure of this basin by continental convergence accompanied by subduction caused arc type volcanism and the deposition of Middle and Upper Birbir Group 650 m.y. ago.

The rocks in the mapped area form part of the Upper Birbir group. The environment of deposition of the rocks ranged from subaerial to subaqueous.

Support for this includes the presence of cross-bedding, graded bedding, presence of conglomeratic unit and absence of well stratified pyroclastics. The dioritic bodies which outcrop continuously and follow north-south direction, may probably outline a young irregular paleo-landscape.

The presence of conglomeratic unit suggest an unconformity characterized by major hiatus before the deposition of the younger rocks. The younger rocks, however, show no sharp contact between the units thereby suggesting continuous volcanic activity and rapid sedimentation. This continuous volcanic activity and accompanied sedimentation is indicated by the presence of intermediate silicic metavolcanics (andesitic - dacitic - rhyolitic tuffs), lapelli tuffs, probably agglomerates and a vast amount of volcano-clastics, and by the presence of blue quartz porphyry.

CHAPTER III

ORE PROSPECTING

3.1. Introduction

The thick soil cover (20-40 metres) and the poor exposure of bed rocks make the area difficult to study geologically. This problem coupled with the occurrence of gossaniferous bodies about the soil cover at different localities encouraged the use of geochemical exploration techniques to understand and detect possible economic sulphide deposits. From time to time the United Nation Mineral Survey and the Ethiopian Institute of Geological Surveys carried out geochemical exploration work on stream sediments bed rocks, soils and gossaniferous bodies. For a better understanding of the mineralizations, diamond, Atlas Copco and manual auger drillings were carried out in Katta at different localities and the work have met mixed fortunes.

3.2. Regional Geochemical Survey

Geochemical survey was first introduced in Ethiopia by United Nations Mineral Survey in 1968. The first works were done in two selected areas, one in Sidamo and the other in Wollega. During the first stage of the exploration, the geochemical survey was primary concerned with collection of stream sediment samples. Analytical results were compiled and included in the UN report (United Nations - Ethiopia, Report on Mineral survey in Two selected Areas of Ethiopia - 1971). Soil samplings were done on the

the subsequent stages. The results of the regional geochemical survey in Western Wollega carried out in the period between 1968 and 1971 are shown in figures 25 and 26. As can be seen from the two figures, Katta falls in the zone delineated to be anomalous in copper arsenic and cobalt. As to the zinc, however, since the high zones are widely spread all over the survey area, no outstanding zone has been indicated.[14]

3.3. Local Geochemical Survey

3.3.1. Stream Sediments

Stream sediment sampling in Katta was the first geochemical survey carried out by United Nations Mineral Survey in the period between 1968-1971. Afterwards several samples were collected by different peoples. The compiled data was statistically treated by Pisarski and presented in a histogram figure 27. The statistical interpretation, however, fails to show any anomolous value in copper in stream sediment samples draining the Katta 1 and Katta 2 mineralized areas. To know the reason a PH survey was done and it was found out that the reason for small anomalous values was due to the relatively low PH (5.5 - 6.0) of the stream waters which act as dispersant.[15] Therefore, it seems that stream sediment sampling is unimportant in Katta. However, recent very detailed stream sediment sampling indicated what could be interpreted as small pockets of copper mineralization.[14]

3.3.2. Bed Rock and Float Samples

Several rock sampling were done from time to time by different people including the author. The samples are crushed to less than 80 mesh size and 0.25 gm. of it was treated with 1 ml $HClO_4$ heated to white fume and later leached with 9 ml (1 + 9) HCl. Analyses for copper, zinc, nickel, lead and cobalt were performed by atomic absorption. The threshold values of the elements were calculated and the results are presented graphically by histograms (figures 28-32). The variation of the elements with the stratigraphy is shown in Table 9.

The copper, zinc and nickel values in PPM of a number of ferruginous outcrops and float samples of unknown lithology around Borokis river are given below: (Table 10).

Table 9

Rock Types	No. of Samples	Average				
		Co	Co	Ni	Cu	Zn	Pb
Granite	1	7	7	2.5	94	38	19
Quartzo-feld. schist	10	7	7	10	95	63	18
Quartz-sericite phyllite	16	16		26	58	99	21
Quartz-graphitic phyllite	5	27		47	63	100	20
Calcareous-quartz sencite phyllete	17	26		62	65	110	20
Calcareous chlorite schist	5	34		44	85	72	18
Gneiss	1	12		2.5	330	247	44
Metadiorite	1	20		60	70	50	20

The copper, zinc and nickel values in ppm of number of ferruginous outcrops and float samples of unknown lithology around Borokis river are given below:

Table 10

No	Cu	Zn	Ni
1	310	190	330
2	600	105	215
3	100	1300	215
4	330	460	50
5	150	640	375
6	550	510	80
7	360	310	125

The zinc/copper ratio for the different rocks doesn't show any clear pattern of distribution. However, from the table above an upward general decrease of copper and zinc is observed. The Cu-Zn-Pb weight percentage plotted in a ternary diagram, fig. 33 shows that all the rocks fall along or near the Cu-Zn line, thereby suggesting that the rocks are enriched in Cu-Zn and deficient in Pb. This fact well agrees with those obtained from soil data discussed later on.

For establishing the relationship between Co, Cu, Zn, Pb and Ni Spearman Coefficient of rank correlation[42] was applied for 42 rock and 7 gossan analysis.

$$\hat{\rho} = 1 - 6\left(\frac{\sum d^2 + d^2}{n^3 - 1}\right)$$

Where $\hat{\rho}$ = estimate of rank correlation coefficient

d^2 = sum of square differences between the corresponding ranks

n = the number of analysis

$d^2 = 1/12 \sum (l_t^3 - l_t)$ = additional coefficient for the equal analysis values,

m = the number of groups of the equal values

l_t = the number of population members with equal values

Calculated is compared with acceptable

($\hat{\rho}_{acc} = \frac{1.96}{\sqrt{n-1}}$) for 5% level of significance.

The calculated correlation coefficient for each rock types are:

I. Population of 5 analysis calcareous chloritic schist

$\hat{\rho}$ Cu-Zn = 0.904

$\hat{\rho}$ Cu-Co = 0.903

$\hat{\rho}$ Cu-Pb = 0.516

$\hat{\rho}$ Zn-Pb = 0.47

$\hat{\rho}$ Cu-Ni = 0.13

$\hat{\rho}$ Zn-Ni = 0.016 $\hat{\rho}_{acc}$ = 0.98

$\hat{\rho}$ Co-Ni = 0.32

$\hat{\rho}$ Pb-Ni = 0.71

II. Population of 17 analysis of calcareous quartz sericite phyllite

$\hat{\rho}$ Cu-Zn = -0.147

$\hat{\rho}$ Cu-Pb = 0.28

$\hat{\rho}$ Zn-Pb = 0.02

$\hat{\rho}$ Cu-Ni = -0.069 $\hat{\rho}_{acc}$ = 0.49

$\hat{\rho}$ Zn-Ni = 0.65

$\hat{\rho}$ Cu-Co = 0.49

III. Population of 5 analysis of quartz-graphitic phyllite

$\hat{\rho}$ Co-Ni = -0.25

$\hat{\rho}$ Co-Cu = 0.903

$\hat{\rho}$ Co-Zn = -0.25

$\hat{\rho}$ Co-Pb = 0.52

$\hat{\rho}$ Ni-Cu = 0.52

$\hat{\rho}$ Ni-Zm = 1 $\hat{\rho}_{acc}$ = 0.98

$\hat{\rho}$ Ni-Pb = 0.61

$\hat{\rho}$ Cu-Zn = 0.52

$\hat{\rho}$ Cu-Pb = -0.25

$\hat{\rho}$ Zn-Pb = 0.61

IV. Population of3 analysis of quartz-sericite phyllite

$\hat{\rho}$ Co-Ni = 1

$\hat{\rho}$ Co-Cu = -0.7

$\hat{\rho}$ Co-Zn = 1

$\hat{\rho}$ Co-Pb = -0.7 $\hat{\rho}_{acc}$ = 1.0

$\hat{\rho}$ Ni-Cu = -0.7

$\hat{\rho}$ Ni-Zm = 1

$\hat{\rho}$ Ni-Pb = -0.7

$\hat{\rho}$ Cu-Zn = -0.7

$\hat{\rho}$ Cu-Pb = 1

$\hat{\rho}$ Zn-Pb = 1

V. Population of 10 analysis of quartzo-feldspathic schist

$\hat{\rho}$ Co-Ni = 0.325

$\hat{\rho}$ Co-Cu = 0.63

$\hat{\rho}$ Co-Zn = 0.02

$\hat{\rho}$ Co-Pb = -0.178

$\hat{\rho}$ Ni-Cu = 0.041 $\quad \hat{\rho}_{acc} = 0.69$

$\hat{\rho}$ Ni-Zn = -0.24

$\hat{\rho}$ Ni-Pb = -0.14

$\hat{\rho}$ Cu-Zn = 0.37

$\hat{\rho}$ Cu-Pb = 0.92

$\hat{\rho}$ Zn-Pb = 0.705

VI. Population of 6 analysis of ferruginuous outcrops 9 float samples.

$\hat{\rho}$ Cu-Zn = -0.45

$\hat{\rho}$ Cu-Ni = -0.62 $\quad \hat{\rho}_{acc} = 0.875$

$\hat{\rho}$ Zn-Ni = 0.16

The results are plotted in fig. 34-39. Good correlation is maintained between Cu-Zn and Co-Cu.

In order to establish how significant are differences of $\bar{x}$ and s for different rock types Fisher $F = s_1^2/s_2^2$ and student t[43]

$$t = \frac{(\bar{x}_1 - \bar{x}_2) - (N_1 - N_2)}{s_p \sqrt{1/n_1 + 1/n_2}}$$

Where $\bar{x}$ = sample mean

N = population mean

n = sample size

and $s_p^2 = \frac{(n_1 - 1)s_1^2 + (n_2 - 1)s_2^2}{n_1 + n_2 - 2}$

Where s = standard deviation

Criteria were applied.

The confidence interval for $F = \frac{s_1^2}{s_2^2}$ with 5% level significance and $k_1 = n_1 - 1$ and $k_2 = n_2 - 1$ degree of freedom is taken from Fisher criterion table. The confidence interval for $t = \frac{x_1 - x_2 - N_1 - N_2}{s_p \sqrt{1/n_1 + 1/n_2}}$ with 5% level of significance and $k = n_1 + n_2 - 2$ degree of freedom is taken from student t criterion table. F and t distributions with their corresponding degree of freedom and values for each rock type are shown below.

I. Calcareous-quartz sericite phyllite (A) Vs quartz-graphite phyllite (B).

$F_{Cu} = \frac{S^2 Cu\ A}{S^2 Cu\ B} = 4.68 < 5.87$ degree of freedom

$F_{Zn} = \frac{S^2 Zn\ A}{S^2 Zn\ B} = 0.797 < 5.87 = 5.87$

$t_{Cu} = 0.049 < 2.086$

$t_{Zn} = 0.357 < 2.086$ degree of freedom = 19.4

II. Cal-qz-ser-phyllite (A) Vs qz-ser-phyllite (C)

$$F_{Cu} = \frac{S^2 Cu\ A}{S^2 Cu\ C} = 1.605 < 19.4$$

$$F_{Zn} = \frac{S^2 Zm\ A}{S^2 Zn\ C} = 13.86 < 19.4$$

degree of freedom = 19.4

$t_{Cu} = 0.015 < 2.101$

$t_{Zn} = 0.462 < 2.101$ degree of freedom = 2.101

III. Cal-qz-ser-phyllite (A) Vs cal-chloritic schist (D)

$$F_{Cu} = \frac{S^2 Cu\ A}{S^2 Zn\ D} = 0.392 < 5.87$$

$$F_{Zn} = \frac{S^2 Zn\ A}{S^2 Zn\ D} = 2.93 < 5.87$$

degree of freedom = 5.87

$t_{Cu} = -0.85 < 2.086$

$t_{Zn} = 1.76 < 2.086$ degree of freedom = 2.086

IV. Cal-qz-ser phyllite (A) Vs quartzo-feldspathic schist (E)

$$F_{Cu} = \frac{S^2 Cu\ A}{S^2 Cu\ E} = 0.377 < 3.00$$

$$F_{Zn} = \frac{S^2 Zm\ A}{S^2 Zn\ E} = 0.519 < 3.00$$

degree of freedom = 3.00

$t_{Cu} = 0.046 < 2.060$

$t_{Zn} = 2.32 > 2.060$ degree of freedom = 2.060

Thus calculation of F and t for Cu and Zn suggest that there should not be significant t difference between $\bar{x}$ and s for these elements in different rocks. Infact the same conclusion is reached in phyllites and schists in adjacent area.

Again to determine if there is any lateral change westward in the elements, calculations done on the different rock types discussed above are compared with the calculations done by Soukourokov on phyllites and greenschists of Katta 2. The results show no significant difference laterally in the elements within either the phyllites or greenschists but a slight increase in Zn content eastward is observed. This is confirmed by Soukourkorv's calculations on 575 bedrock and 377 float samples in which the Zn/Cu ratio shows definite pattern of distribution laterally, i.e., lateral zonation. The boundary between the high values of Cu and Zn runs approx. north east[44] (see fig. 40).

From the above calculations it can be concluded that the actual surface distribution of the elements is not controlled by any specific lithological unit. The same conclusion is reached by Soukourokov and to support his conclusion he established orientation pattern for gossaniferous zone and noted that the gossaniferous zones are not related to any particular lithological bed, but cross

Fig. 40

Gossan

GEOCHEMICAL CONTOUR

boundary between Cu & Zn high values

(After Soukorokov, unpublished)

1-12 SAMPLE SITES

3.3.3. Soil Samples

The first geochemical soil survey was done at Katta 1 by UN in 1971 during which a 50 meter wide anomalous zone was established across the strike of mineralization. Because of this later work started and succeeded to delineate a 300 metre long and 100 metre wide anomalous zone. The result thus obtained encouraged different people to cover almost the whole Katta by soil sampling in regular grids. The author also collected a minimum total of 600 soil samples from three different localities. Tuluboli, Enemay and Aderie. The samples are sent to the Geochemical Laboratory in Addis Ababa. 250 mg of the samples was put into a test tube (180 by 16 mm) and 1 ml of 60-70% $HClO_4$ (perchloric acid) was added, and digested on sand tray for 30-45 minutes then 9 ml (1+9) HCl was added and subsequently shaken. The solution was then heated in water both for 5-10 minutes. Finally it was removed and shaken for complete mixing and was let stand overnight. It was then read on the atomic absorption spectrophotometer caliberated by using standard solutions. The results obtained are presented in histograms (see figures 41-45). The range in PPM, the threshold values of each element analyzed and the highest values obtained for soils collected from Enemay, Borokis Aderie and Tulu Boli areas are tabulated (see Tables 11-14). To calculate

the threshold values the formula: Tr = X+2S (where X is mean and S is standard deviation) is used. Geochemical maps for Tulu Boli and Borokiss are also prepared for each element (see figures 46-57). Profile sections of Tulu Boli, Enemay and Aderie areas are also made (see figures 58-60).

Enemay Area (Profile 1)

	Cu	Zn	Co	Ni	Pb
Range in PPm	2.5-130	25-100	2.5-110	2.5-420	10-55
Threshold	111.4	66.4	52	292.2	29
Highest values	130	100	110	420	55
	115	90	100	350	45
	120	85	95	385	40
	110	80	90	380	30
	105	75	85	360	25

PPm

Table 11

Aderie Area (Profile 2)

	Cu	Zn	Co	Ni	Pb
Range in PPm	10-90	30-110	15-45	35-125	20-40
Threshold	88.7	98	36	87	38
Highest values	90	110	45	125	40
	85	100	40	120	35
	80	90	35	115	30
	75	80	30	110	25
	70	75	25	100	20

Table 12

Tulu Boli Area (Profile 3)

	Cu	Zn	Co	Ni	Pb	As*
Range in PPm	40-115	30-105	15-170	50-300	20-81	12-548
Threshold	80	70	40	160	60	150
Highest	115	105	170	300	81	548
values	105	90	55	270	77	473
	100	85	50	240	75	434
	95	80	45	220	71	415
	90	75	40	210	70	384

(*As data obtained from Sisay, 1972) - Table 13.

Borokissa (Analytical Data obtained from Sisay & Hailu 1972)

	Cu	Zn	Co	Ni	Pb	As
Range	35-113	12-196	42-78	46-159	26-80	21-455
Threshold	80	100	65	100	40	150
Highest	113	154	78	159	80	455
values	96	118	74	137	67	405
	85	115	74	124	64	376
	84	113	74	114	62	344
	83	111	74	113	62	300

Table 14

Apart from the tables given above, soil samplings at Katta proper show the following Cu results (only highest values are given)[17].

Katta 1 = 10,900 PPm	Katta 3 = 700 PPm	Kutala = 770 PP
Katta 2 = 3,200 "	Katta 6 = 1,300 "	Tuluchuche = 32
Katta 2 South = 1,410 PPm	Katta N.W. = 500 "	Katta S.W. = 55

The results and geochemical maps show that the dispersion pattern of the elements is not continuous and the anomalous zones are found as separate patches in any one of the localities.

At Tulu Boli and Borokiss the anomalous zones trend north-south following the strike and foliation plane. The ZnxAgxPb/CoxNixCu ratio of all the soil samples from Tulu Boli, Enemay and Aderie area is below 1 thereby disturbing the lateral zonation pattern in which relatively mobile elements (Zn, As & Pb) become prominant towards the east (fig. 40). The relating higher Co, Ni, & Cu content may be due to the many dicritic intrusions, found north east of the mapped area, in which high Ni anomalous zone is delineated (fig. 26).

3.3.4. Drilling

Recently drilling operation was carried out in the year 1972-78 by United Nations and it is still being continued at the time of the preparation and writing of this thesis.

3.3.4.1. Introduction

According to Ahmad a minimum total of 205 boreholes (Atlascopoco and manual auger drills in about 33 profiles, each profile consisting of 2 to 26 boreholes of varying depth and reaching a maximum of 45 metres, were dug in the past years.[17] In addition, a minimum total of 9 BBs type diamond drill holes were dug. Some of the drill hole sites are shown in fig. 61. The maximum depth attained is in DDH_7 (225 metres). Here BBs type 2 drilling was employed using bit size NX to 44 metres, BX to 162 metres and then AX to bottom.

3.3.4.2. Sampling System

There is no regular spacing practiced during sampling operations. The spacing could vary depending on three factors.

(i) intensity of weathering

(ii) " of mineralization

(iii) variation in lithology

The greater the intensity of weathering, wider the spacing and greater the intensity of mineralization, closer the spacing. For the same lithology, the spacing is wider and whenever quick variation occur, the spacing becomes closer. This being so, in diamond drill hole

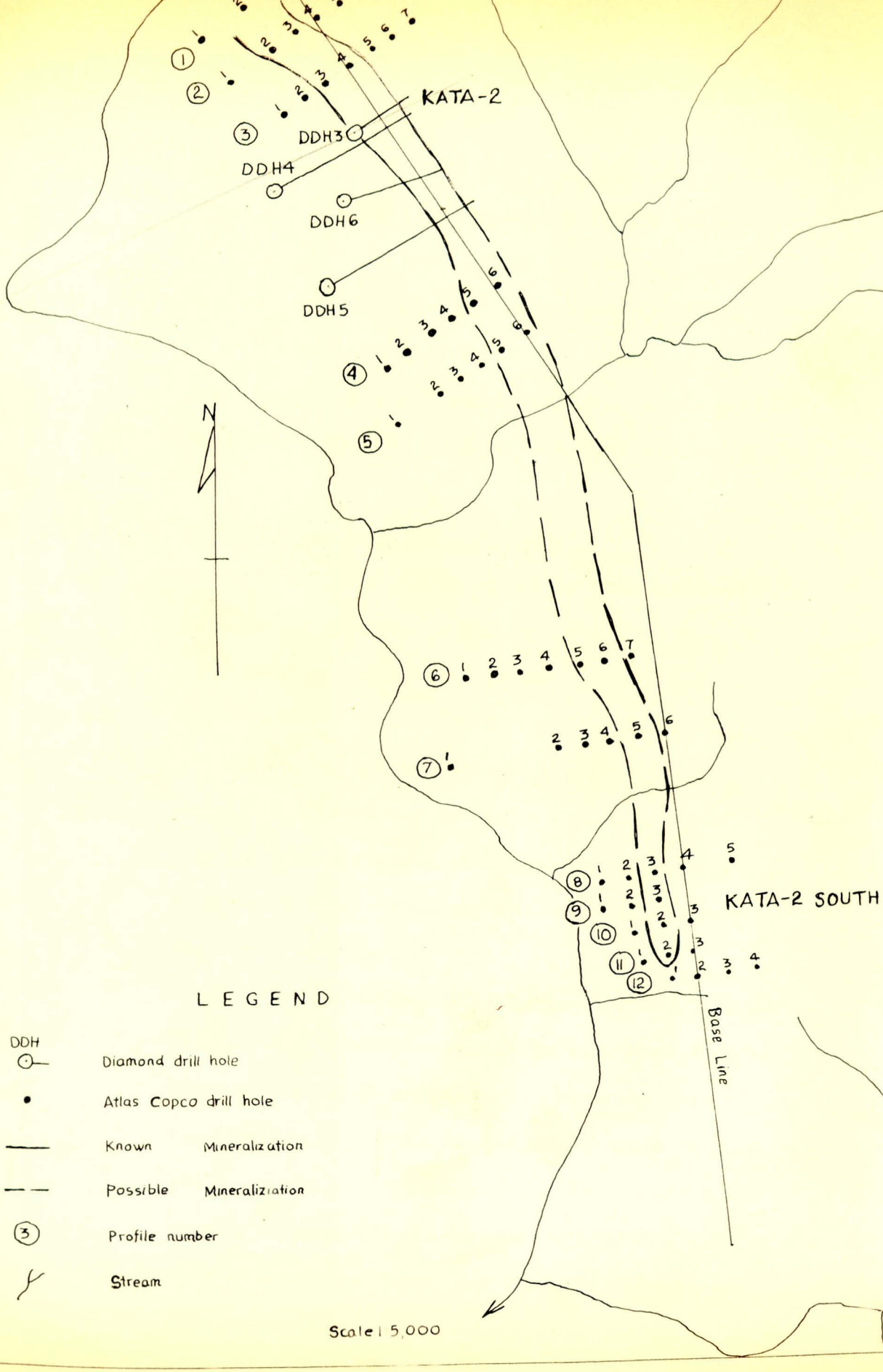
KATA-2
DDH3
DDH4
DDH6
DDH5
N
KATA-2 SOUTH
Base Line
LEGEND
DDH
Diamond drill hole
Atlas Copco drill hole
Known Mineralization
Possible Mineralization
Profile number
Stream
Scale 1:5,000

numbered 3, 4, 5 and 6 one metre interval on the average, between two successive sample takings is observed. In hole number 7, however, sludge samples were collected at 5 metres intervals.

The sampling system is not consistent, and doesn't seem logical and scientific. This therefore presents some problem in the final conclusion.

3.3.4.3. Analysis and Data Presentation

The samples are analyzed by atomic absorption spectro-photometry for Cu, Zn, Pb, Co & Ni. In the analysis the same procedure is used here as that used for surface soil. The data are then statistically treated to see if there is co-relation between the elements analyzed. The results are presented in scatter diagram (see figures 62-64). Good corelations are obtained for Cu-Zn and Cu-Co.

The Cu-Zn-Pb percentages for two drill holes (DDH_4 & DDH_6) are calculated to see which type of mineralization is dominant in the area. The results are presented in ternary diagram (fig. 33). It can be seen from the diagram that the area is enriched in Cu-Zn and deficient in Pb mineralizations. From the diagrams as well as from chemical analysis data copper by far

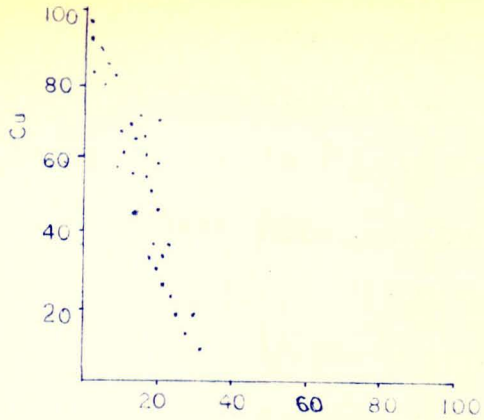

FIG.62

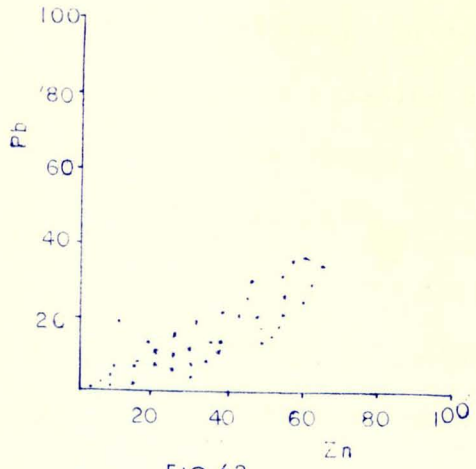

FIG.63

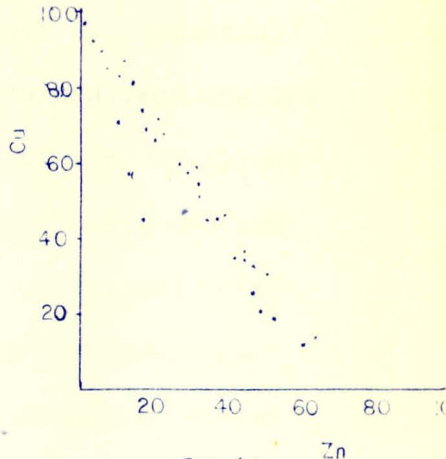

FIG.64

exceeds zinc in assay values. The highest copper assay values against number of occurrence for each drill hole is shown in the histograms in fig. 65-69.

3.3.4.4. Depth Variation

According to Ahmed[17] a maximum of 27,000 PPm (2.7%) of copper was found in profile number 3 at a depth of 24 metres. Regarding zinc values, 450 PPm at 11 and 14 m depths was found from profile 4. Otherwise the values of zinc are lower and the anomalous zone narrower. Slight indications of lead and silver, and unimportant but relatively higher values of nickel and cobalt are observed.

Basing upon the results obtained from shallow drillings, a number of BBs type diamond drillings at 45° inclination with 60° azimuth were carried out. The depth variation for each diamond drill hole is discussed below. The percent recovery differs for different rocks but generally varies between 85-95% on the average.

(i) DDH_3

In this drill hole a maximum depth of 45 m is reached. The 25-45 metre depth can be treated as anomalous in Cu and Zn. About 5.5% and 7.8% Cu values with about 95% recovery are obtained from depths of about

28 metre and 35 m respectively from errru-ginuous silicified rocks and sericite-chlorite-talc schists. After 35 metre mark, however the value falls down to 2%.

(ii) DDH 4

In this hole, between 130-187 m. depths anomalous values of copper are obtained. At a depth of 164 metres, 2.3% Cu is seen in siliceous marble with 95% recovery. Below the 187 m mark, however, a very sharp decrease upto No. 003%) in Cu values is observed. The Zn values on the other hand, excepting the very high and very low values every now and then, are more or less constant and uniform. The maximum value is obtained from calcareous schists at 120 m. depth with 90% recovery. Low zinc values (110 PPm on average) are seen in amphibolites. The overall calculated average value for copper is 0.86% and Zn 88 PPm.

Ni values decrease with depth, from 340 PPm at 63 m. depth to 28 PPm at 211 m. depth. Pb, Co & (As) are uniform throughout, with average PPm of 22, 40 & (30) respectively.

(iii) DDH_5

The copper value is low (No. 15%) on the average. However, high sharp anomalies upto 1.18% are found at depths between 140-145 m. in undifferentiated greenschists and amphibolites with 90-100% recovery. Below 145 m, the copper content decreases with depth.

Fairly high values of zinc are observed between 125 m and 156 m depth with values between 100 and 500 PPm in undifferentiated greenschists (chlorite schist and amphbole) with about 80% recovery on the average. There is a general gradual increase in Zn values upto 156 m. depth. Below this depth, however, more or less constant value is seen.

The Ni content shows no significant varation with depth.

(iv) DDH_6

There is a general increase in copper values upto a depth of 94.21 m. at which depth more than 1% Cu is obtained in chloritic schist with 95% recovery. Thereafter upto 110 m. mark, there is a decrease in value.

At 110 m. depth a sharp rise (0.63%) is seen in undifferentiated schists and amphibolites with 92% recovery. A decrease, however,

The zinc values are more or less constant (100-200 PPm) upto a depth of 110 m. where more than 300 PPm is observed. Below this mark, in the same unit, the values oscillate between 100 and 250 PPm.

Ni slightly increases with depth (average 19 PPm) whereas Pb, Co and As are uniform with average PPm of 50, 35 and 18 respectively.

(v) $\underline{DDH_5}$

Quantitative chemical analysis of sludge samples showed the copper content to range from 74 to 1100 PPm. The maximum value is obtained from clastic sericite chlorite schist at a depth of 70 m. Thereafter there is a uniform but lower values are observed.

CHAPTER IV

MINERALIZATIONS

4.1. Ore Petrography

Two types of studies are made to study the type, texture and structure of ore minerals: studies made on crushed samples and studies on polished sections.

4.1.1. Crushed Samples

Eleven representative rock samples from each stratigraphic unit in the mapped area are crushed to 1 mm size, panned to separate the ore minerals from the unwanted gangue minerals and studied under binocular microscope to determine type of ore minerals.

The results are given below:

Sample No.	Ore Minerals
10/1390	Magnetite (2%), chalcopyrite, pyrite (1%)
1373	Magnetite (3%), chalcopyrite (1%)
1383	Magnetite + heametite (5%)
1392	Pyrite, chalcopyrite (2%)
1393	Magnetite (30%), pyrite, chalcopyrite (1%
1391	Magnetite
1394	Magnetite (40%), pyrite (2%)
1388	Magnetite (35%)
1396	Magnetite (2%), pyrite, chalcopyrite (3%)
1398	Magnetite (40%), pyrite, (7%) limonite (coating)
1395	Pyrite (40%), chalcopyrite (10%)

The modal average percentage calculation shows that 60% of the ore minerals is magnetite and remaining 40% sulphides.

4.1.2. Polished Sections

To study the type of ore minerals, their texture and structure reflected light ore microscopy has been carried out. The following minerals have been identified: sulphides: pyrite, sphalerite, pyrrhotite, chalcopyrite, cubanite, bornite; sulphosalts: bournonite; and oxides: cuprite, haematite and magnetite. The different properties, structure and texture, the association ofeach of the minerals are discussed below.

Pyrite

Polishing Properties

Pyrite (FeS_2) is abundantly found in the rocks of the area. Pyrite is difficult to polish and very often it yields uneven surfaces only. However after careful and prolonged polishing using abrasvies and different soft clothes, excellent polished surface is attained.

Reflection Behavior

Reflectivity is very high and its colour is very light yellow. Anisotropic effects are not seen under crossed nicols.

Deformations

Deformations caused by tectonic stress are seen producing cataclasm in pyrite. It is in places highly

crushed undergoing the same metamorphic history as the enclosing rocks. It also shows microfoldings in places. Apart from this, there is also another generation of recrystallized pyrite in which no deformation is observed where recrystallization is not complete the previous deformed pyrite remains at the rims.

Structures

The first generation of pyrite (the highly deformed and unrecrystallized one) shows banding and follows the foliation and bedding planes. Sometimes microfoldings are observed. The recrystallized pyrite is sometimes found filling geodes, silicates occupying the rim and pyrite the centre thereby showing pyrite is the last to crystallize. This pyrite is epigenetic (remobilized) that is, rearranged during late metamorphic stages. At other time pyrite is found isolated exhibiting no structure. Veinlets of pyrite cutting the rock's structures are also observed.

Texture

The shape of the recrystallized pyrite is generally idiomorphic. Since this pyrite is not affected by metamorphism it may have attained its crystal form during or immediately after the last metamorphic event.

The grain size of this pyrite vary from 0.1 mm to 0.25 cm. Porphyroblasts of pyrite are also observed. The metacrysts some times noticed have been formed at the expenses of the host minerals as metasomatic replacement. The deformed pyrite, on the other hand, seems to have no crystallic forms and simply stretches as thin films, but careful observation shows very small well shaped (euhedral) recrystallized pyrite.

Replacement and Association

Chalcopyrite, cubanite and pyrrhotite, and also sphalerite are seen associated to recrystallized pyrite. Metacrysts of pyrite frequently observed may be formed due to metasomatic replacement of the mineral in which it is hosted (commonly silicates). Particular relations occur when carbonate is present in chalcopyrite. In such a case, most of the recrystallized pyrite related to cubanite in chalcopyrite and hence a genetic relationship exists. In this case pyrite, probably, must be considered as last product of the unmixing process where cubanite has been separated from chalcopyrite.

Conclusion

There are two generations of pyrite, the first and oldest one occur as highly deformed pyrite which follows the bedding plane and as recrystallized, disseminated individuals. These are considered to be

syngenetic with the rocks. The other types are geode filling and vein types which cross-cut foliation plane. Hence these two are epigenetic.*

The frequent association of especially chalcopyrite with recrystallized pyrite suggest that they are formed during last crystallization phenomena. *Furthermore, the recrystallized pyrite formed at the expense of the layered and deformed one must be considered as an epigenetic evolution of it.

Chalcopyrite

Polishing Properties

Chalcopyrite ($Cu\ FeS_2$) is easily polished and may yeld excellent polished surfaces though the low hardness leads very often to uneven polishing, when associated to hard minerals like pyrite, pyrrhotite etc.

Reflective Behavior

Chalcopyrite is light yellow in colour and has a high lustre. It shows a weak anisotropy under crossed nicols.

Deformation

No deformation is observed in chalcopyrite.

Structures

Chalcopyrite is found mainly scattered throughout the specimens. Sometimes, however, it is found along bedding planes and crosscutting foliation planes as veinlets. In some polished sections chalcopyrite is

seen filling geodes with quartz and prismatic silicates. In fractures of sphalerite (1), chalcopyrite is seen entering thereby showing that it is a late comer.

Texture

The grain size is highly variable. Sometimes quite large (0.25-0.3 cm), may also be very tiny. The shape is also variable out mainly allotriomorphic.

Replacement and Association

For its association see under pyrite. In most studied sections chalcopyrite is seen replaced by bornite. Exsolution of chalcopyrite is seen with both sphalerite and magnetite. Often chalcopyrite shows evidence of formation at temperatures greater than 250^{o}C, by the presence of exsolution lamellae of cubanite.

Conclusion

Just like pyrite, chalcopyrite shows two generations. The syngenetic disseminated type and the egigenetic geode and vein type. In the paragenesis the actual setting of the second chalcopyrite is restricted to late crystallization phenomena.

Sphalerite

Polishing Properties

Sphalerite (Zns) is polished nicely though sometimes it is easily scratched.

Reflection Behavior

Sphalerite has low reflectivity and its colour is gray. It is completely dark under crossed nicols unless internal reflections interfere.

Deformation

No deformation is seen in sphalerite but cracks are present occasionally.

Structures

Sphalerite is seen, just like the other previously described ore minerals, following bedding planes and also scattered throughout the specimen. It is also seen along with chalcopyrite filling spaces between platy silicates.

Texture

The grain size and shape are variable. The size sometimes reaches upto 0.5 cm. The shape is allotriomorphic in the main.

Replacement and Association

For its association see under pyrite often sphalerite carries exsolutions of chalcopyrite and rarely pyrrhotite.

Conclusion

There are two generations of sphalerite. It is the early sphalerite - sphalerite (1) - that makes exsolution with chalcopyrite and pyrrhotite. The late or sphalerite (2) is not seen making

exsolutions and it is observed in drops within chalcopyrite (2). The sphalerite (1) seems to be the most abundant as compared to sphalerite (2).

Pyrrhotite

Polishing Properties

Pyrrhotite (Fes) polished usually excellently with prolonged polishing but in the sections studied it has been very difficult to get good results.

Reflection Behavior

The colour varies from light creamy yellow to brown pink and the reflectivity is fairly high anisotropy is strong.

Deformation

Same as in sphalerite and chalcopyrite.

Structure

Same as in sphalerite.

Texture

Pyrrhotite is generally idiomorphic with grain size reaching upto 0.3 cm.

Replacement and Association

For its association see under pyrite. Pyrrhotite makes exsolution with sphalerite (1).

Conclusion

Pyrrhotite is a recrystallization product and occurs as disseminated throughout the specimen. In some specimen it is found abundantly. In its paragenetic position it is before sphalerite (1).

Bornite

Polishing Properties

Generally bornite (Cu_5FeS_4) is easy to polish and good results have been obtained.

Reflection Behavior

In reflection it has low reflectivity with pinkish brown colour. It has a very weak and variable anisotropy.

Replacement and Association

Bornite is usually associated with cuprite and chalcopyrite. In some sections it is seen replacing chalcopyrite by veins and rims.

Conclusion

Bornite is much more restricted in occurrence. It is related to cementation phenomena in epigenetic types. It is very closely associated with cuprite.

Cuprite

Polishing Properties

Polishing generally seems good but difficult for the hardness of the minerals.

Reflection Behavior

Its colour is generally white grey with strong blue tint. Under crossed nicols it is distinctly anistropic with red internal reflections.

Texture

Cuprite forms well developed hair-thin needles probably in some cases derived from replacement of malachite. The well developed form therefore shows that the mineral grows freely with no interference. Skeleton-like forms of cuprite ore is also observed.

Replacement and Association

Cuprite is restricted to bornite areas so proving a genetic relation.

Conclusion

In its paragenetic position cuprite shares the same history as bornite.

Bournonite

Polishing Properties

Bournonite ($cupbsbs_3$) is easily polished with excellent surface.

Reflection Behavior

Its colour is gray white and its reflectivity medium high. The anisotropy under crossed nicols is distinct.

Texture

The grains are idiomorphic in shape. The grains are seen resting within silicate mass.

Replacement and Association

Because of its restricted and isolated occurrence nothing can be said.

Conclusion

Bournonite is an occasional minerals which probably has been formed as recrystallization of a syngenetic preexisting copper association.

Cubanite

Polishing Properties

Cubanite ($CuFe_2S_3$) takes a good polish without difficulty.

Reflection Behavior

Cubanite is bronze coloured with rather high white content. Its reflectivity is moderately high being between chalcopyrite and pyrrhotite. It has a distinct anisotropy under crossed nicols.

Texture

Cubanite is generally found as lamellae within chalcopyrite. The process of formation can be stated in the following way. At high temperatures much FeS is soluble in $CuFeS_2$ producing high temperature chalcopyrrhotite. Upon cooling this breaks up forming chalcopyrite and cubanite.

Conclusion

Since the unmixing separation of cubanite from chalcopyrite occurs at 250-300°C[45], the existence of cubanite shows those that originally the temperature of formation of the ore must have been over about 250°C.

4.1.3. Summary and Conclusion

The polished sections studies show that there are two types of sulphide mineralization. Syngenetic and Epigenetic types. In the syngenetic type, strata-bound and disseminated sulphide mineralizations are are found. In the epigenetic type, veins and geode fillings are observed.

The syngenetic stratabound type is premetamorphic as there are seen evidences of metamorphism especially in pyrite. Stratabound chalcopyrite and sphalerite are however, recrystallized.

The epigenetic type of mineralization is formed as a result of remobilization of the already existing minerals.

In the remobilization process, the many intrusives in the area might have supplied the necessary heat. A possibility of later introduction of minerals from the intrusive bodies could not be overruled. This epigenet-ic type of mineralization is essentially post metamorphic.

The association of the ore minerals suggest the temperature of formation of the minerals to be over 250°C.

From the mineralogical arrangements and fabrics the following mineral paragenesis is concluded and is presented below according to order of formation.

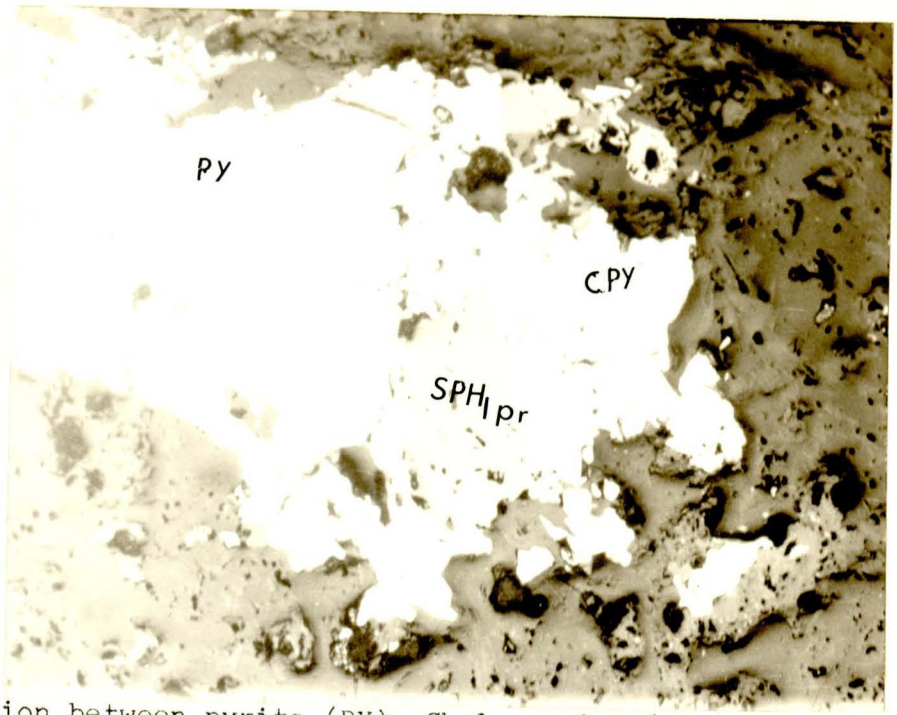

An association between pyrite (PY), Chalcopyrite (CPY), Sphalerite (SPH) and pyrrhotite (Pr). Pyrrhotite occurs at the boundary between Sphalerite and Chalcopyrite. Parallel Nicols. Magnificatic
600 X
Fig. 70.

Strongly deformed pyrite seam (syngenetic). Parallel Nicols
Magnification 600 X
Fig. 71.

Another example of syngenetic deformed pyrite. Parallel Nicols. Magnification 600 X
Fig. 72.

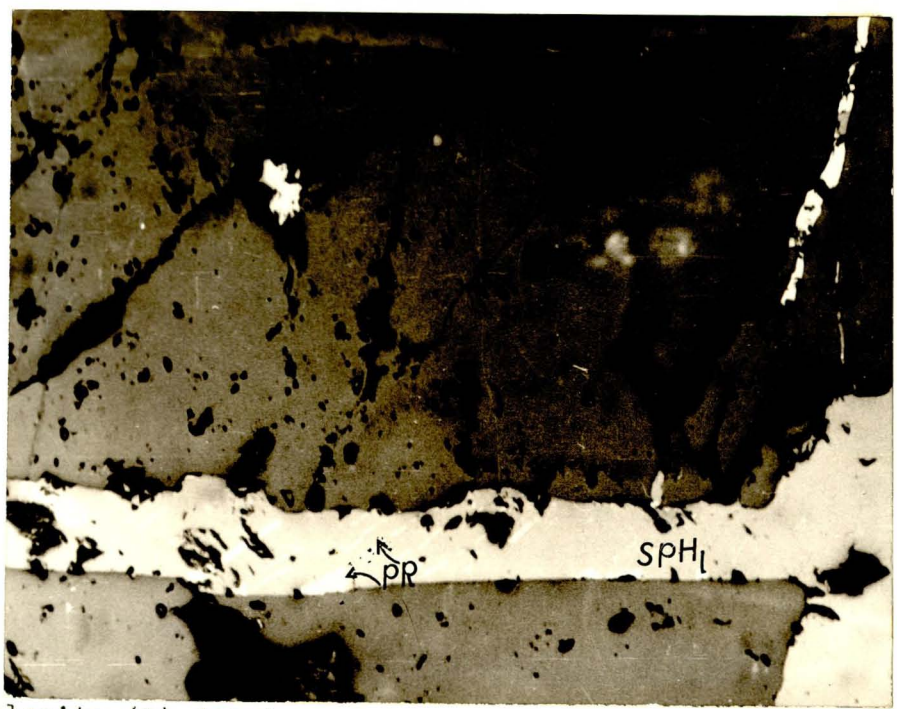

Sphalerite (1) (SPH) with Pyrrhotite (PR) exsolution regularly arranged and Chalcopyrite (CPY) in veinlet in silicates. Parallel Nicols. Magnification 600 X
Fig. 73.

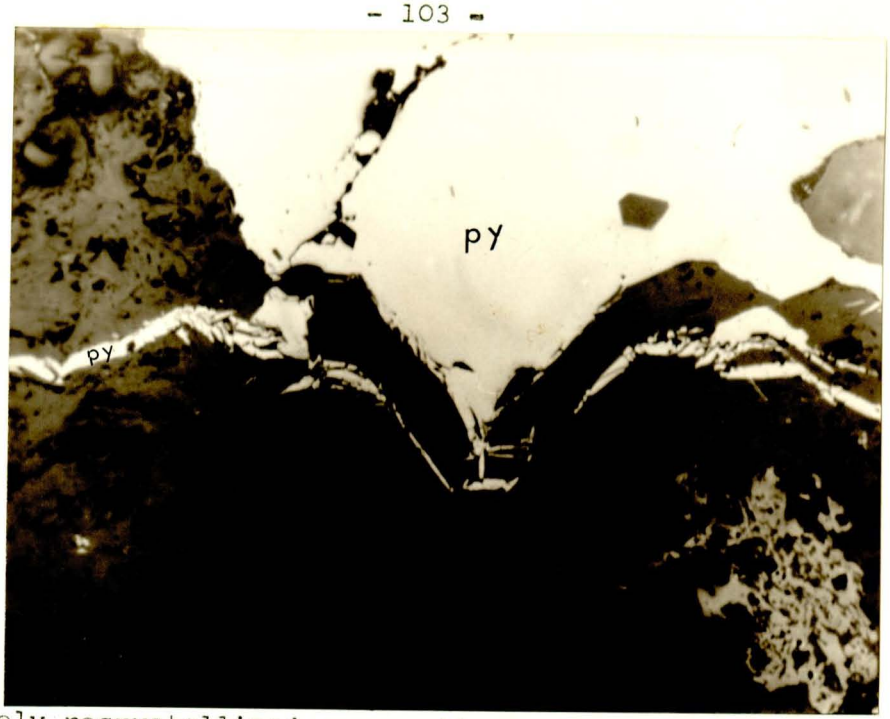

Completely recrystallized syngenetic pyrite. Relict of syngenetic pyrite is seen at the borders. Parallel Nicols. Magnification 600 X
Fig. 74.

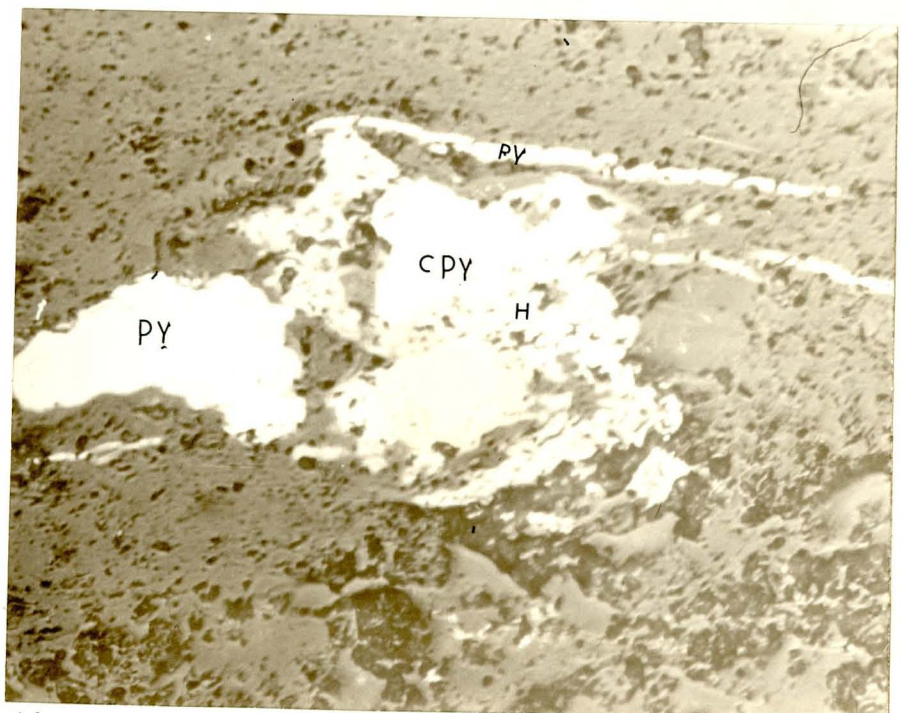

Syngenetic pyrite, (PY) recrystallized pyrite (PY), Chalcopyrite (cPY) and Haematite (H). Parallel Nicols. Magnification 600 X
Fig. 75.

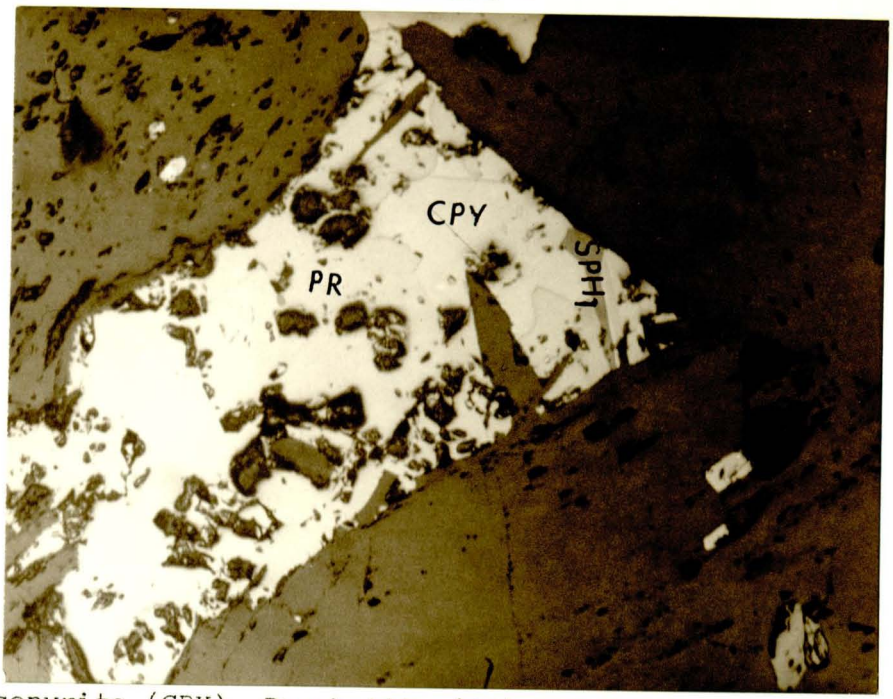

Chalcopyrite (CPY), Pyrrhotite (PR) and Sphalerite (1) (SPH), in gangue minerals. Parallel Nicols. Magnification 600 X
Fig. 76.

Bournonite (BR) grains (anisotropic) with silicate mass. Crossed Nicols. Magnification 600 X
Fig. 77.

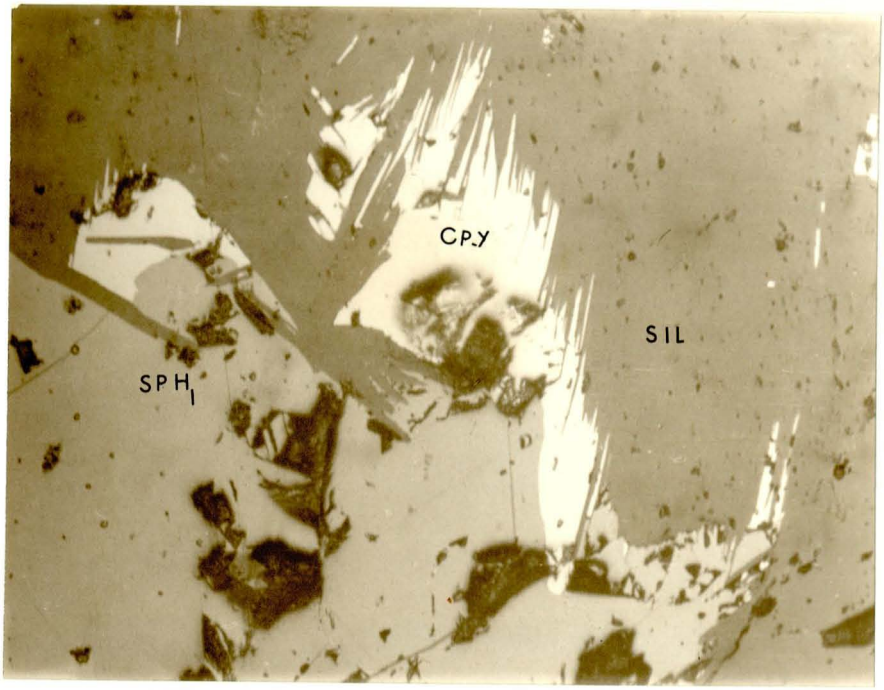

Sphalerite (1) Chalcopyrite filling spaces between platy silicates. Parallel Nicols. Magnification 600 X
Fig. 78.

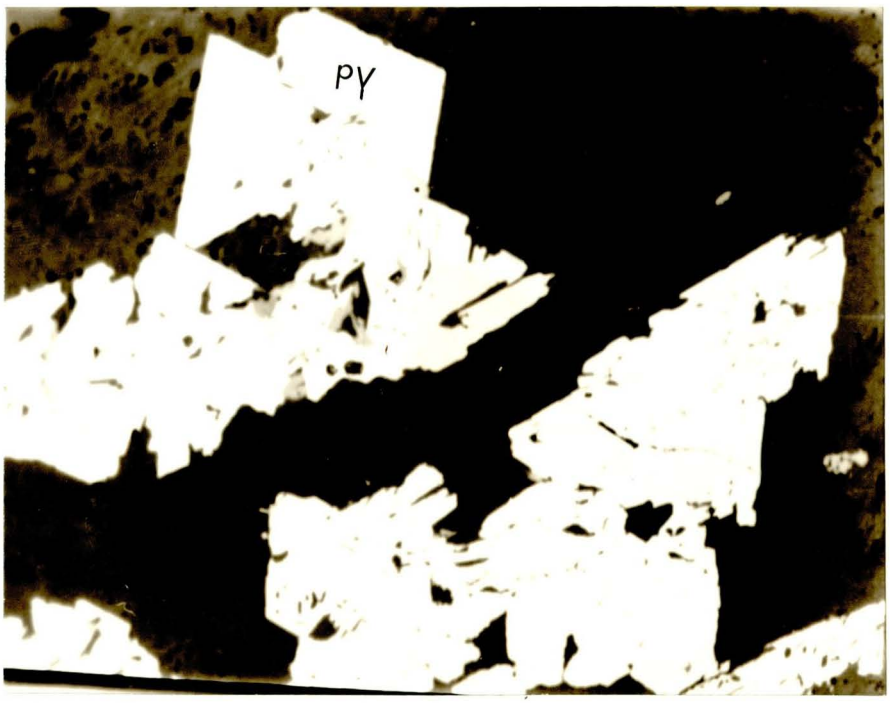

Well shaped recrystallized pyrite crystals. Parallel Nicols. Magnification 600 X
Fig. 79.

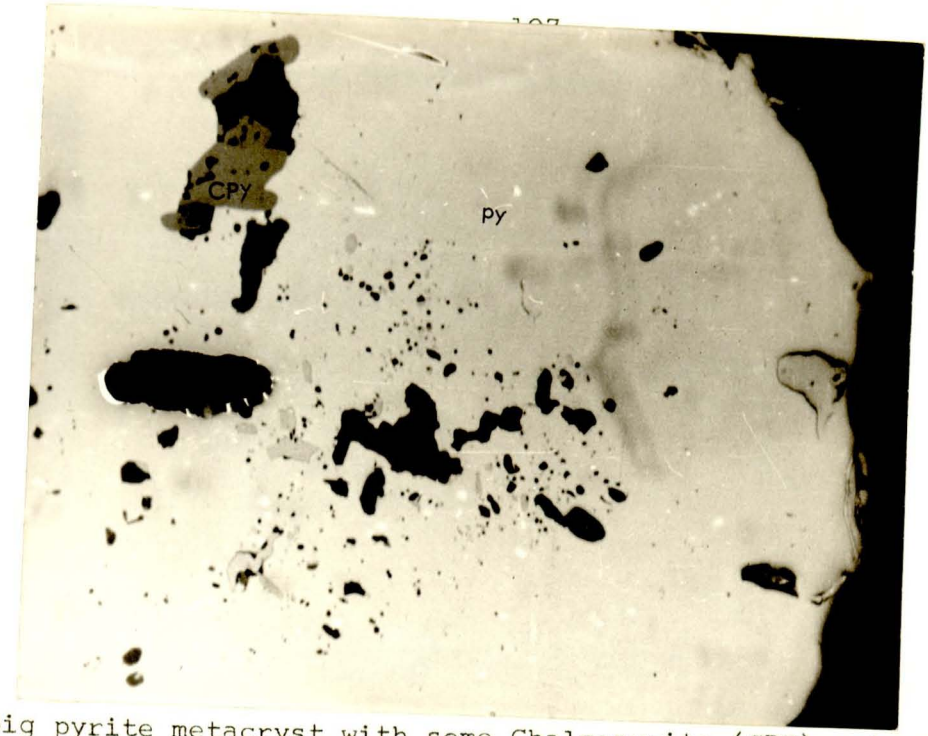

Big pyrite metacryst with some Chalcopyrite (CPY) and relicts of silicate ground mass. Parallel Nicols. Magnification 600 X
Fig. 82.

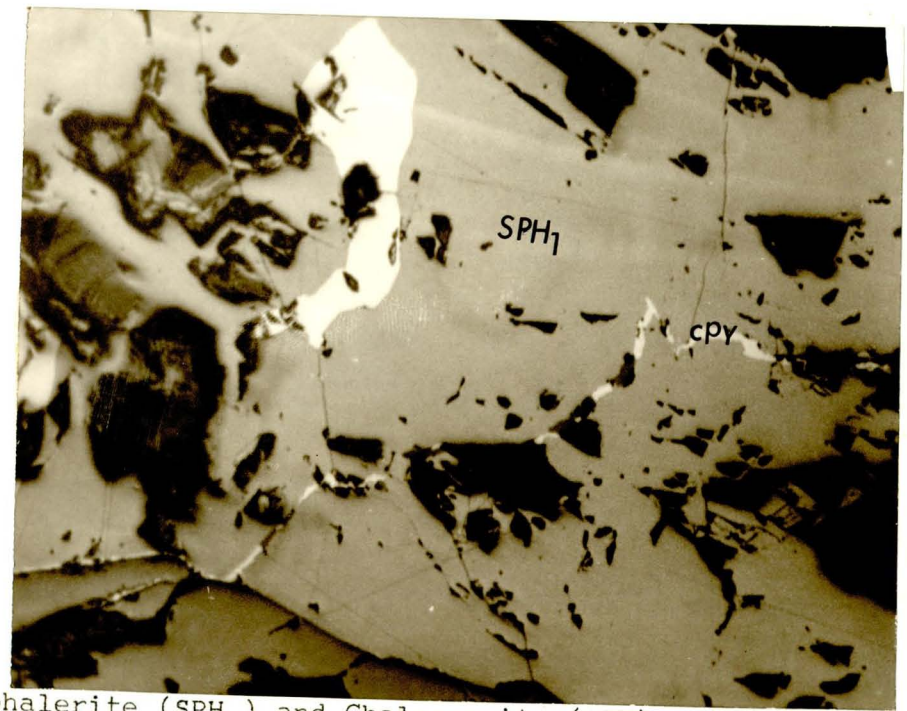

Sphalerite (SPH_1) and Chalcopyrite (CPY) ore veinlet and large area. Parallel Nicols. Magnification 600X
Fig. 83.

Recrystallized pyrite in Syngenetic pyrite and Sphalerite.
Parallel Nicols. Magnification 600 X
Fig. 80.

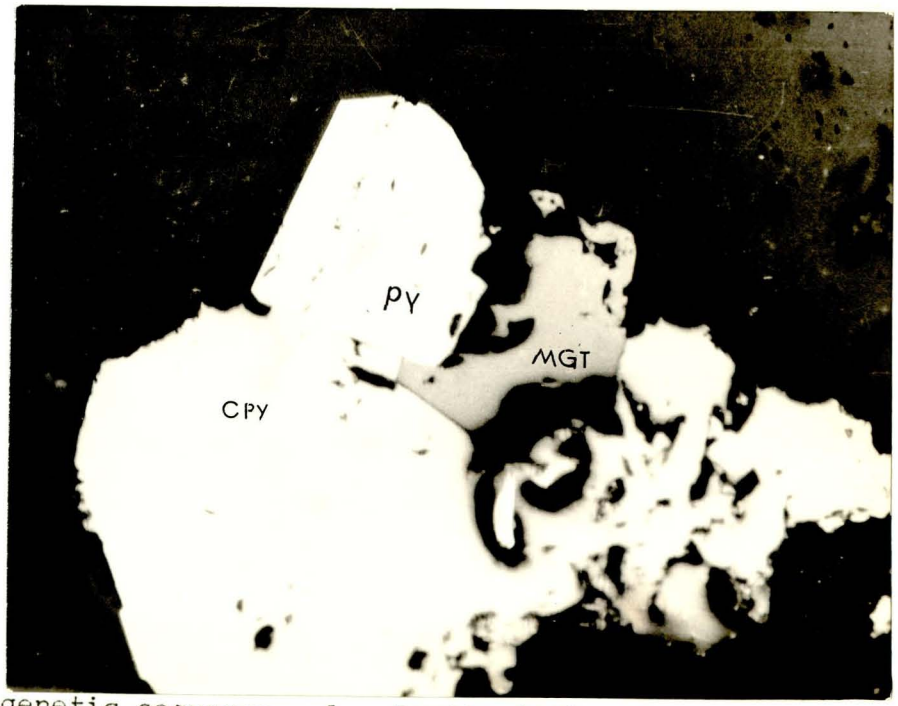

Paragenetic sequence. 1. Pyrite (PY); 2. Magnetite (MGT);
3. Calco-pyrite (CPY) in silicate ground mass. Parallel Nicols.
Magnification 600 X
Fig. 81.

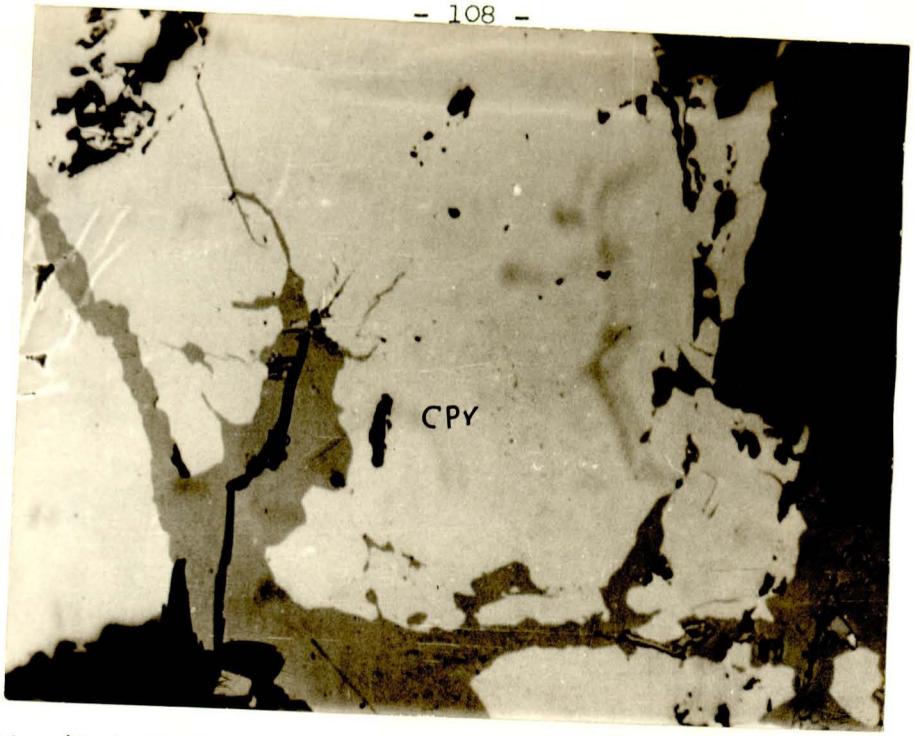

Bornite (Bo) replacement along fractures in Chalcopyrite (cPY) and gangue minerals. Parallel Nicols. Magnification 600 X
Fig. 84.

Cuprite (Cu) in single needles and groups, in Bornite (Bo), replacing Chalcopyrite (cPY) and gangue minerals (black). Parallel Nicols. Magnification 600 X
Fig. 85.

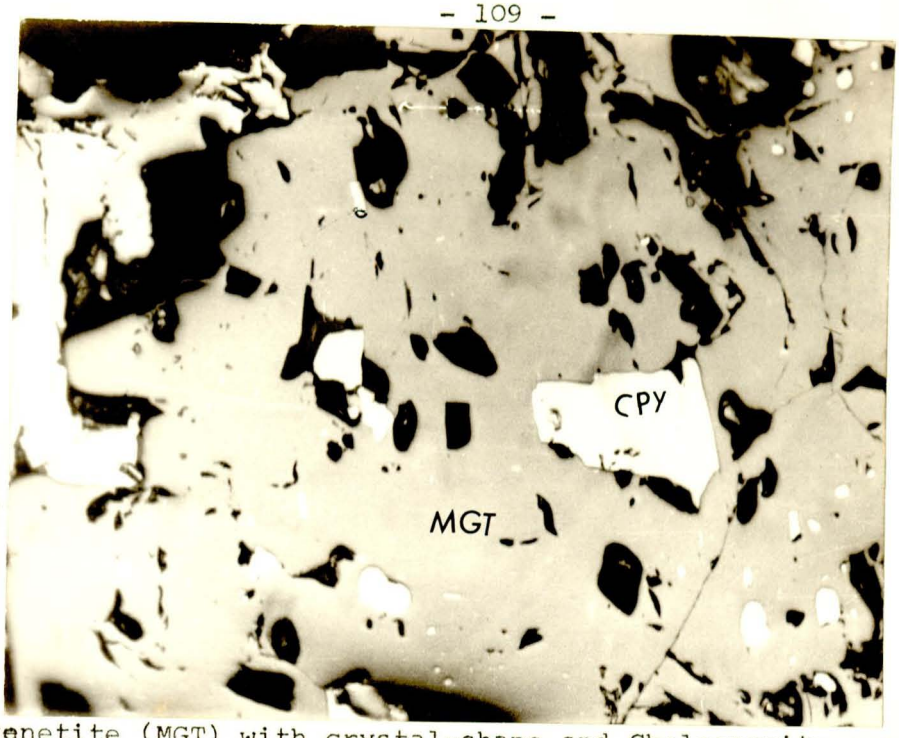

Magenetite (MGT) with crystal-shape and Chalcopyrite exsolutions.
Parallel Nicols. Magnification 600 X
Fig. 86.

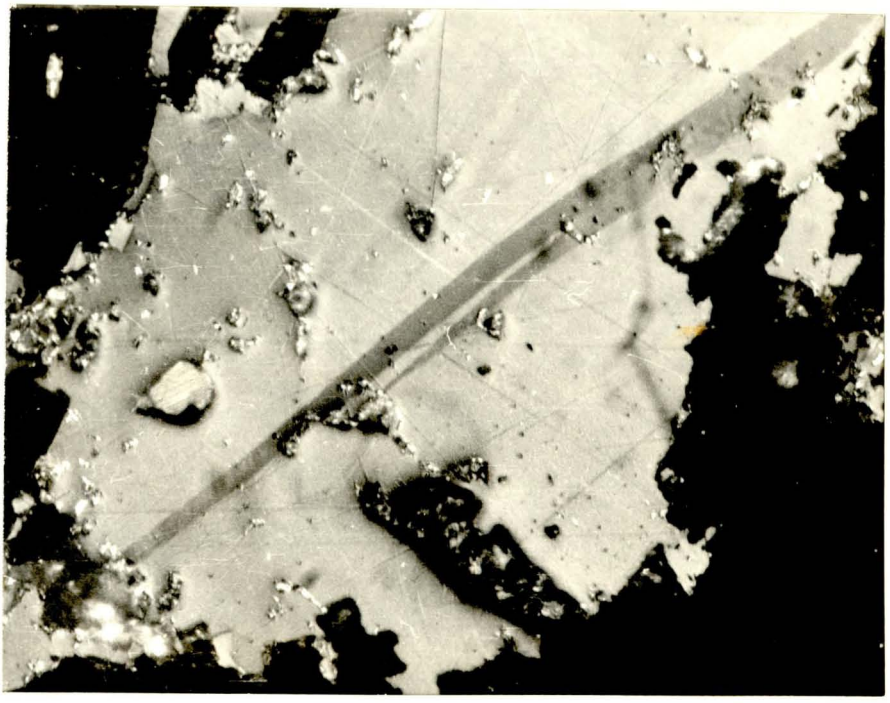

Chalcopyrite with Cubanite lamellae in silicates. Parallel Nicols
Magnification 600 X
Fig. 87.

4.1.3.1. Mineralizing Events

Syngenetic	Epigenetic (Remobilization)
Pyrite (some recrystallized)	Pyrrhotite + (Bournonite)
Chalcopyrite (recrystallized)	Sphalerite (1)
Sphalerite (recrystallized)	Chalcopyrite + Cubanite
Haematite (partly oxidized product)	Sphalerite (2)
	Bornite
	Cuprite
	Haematite

4.2. Depth Relation

Element content variation with depth is seen in fig. 88-89 for drill hole no. 4 & 6. In drill hole 4 there is an upward increase in Zn content and a downward increase in copper content are observed. In hole no. 6 a general increase in copper with depth is clearly seen. Several ratios, $\frac{Znx Pbx Ag}{Cux Cox Ni}$, $\frac{Znx Pbx Ag}{Cux Co}$, $\frac{Znx Pb}{Cu^2}$ and Zn/Cu are calculated to determine the relationship and correlation among the elements. The best result is seen by Zn/Cu ratio for hole no. 4. Upto 74 metre depth the ratio Zn/Cu remains $\geq$ 1. Below 74 m., however, the ratio becomes $<$ 1. The reason for this could be in the differing mobilities of the two elements or in a different abundance of them in the rock units crossed by the bore holes since zinc is highly mobile it is found far from the main mineralized zone. But copper is relatively immobile and is found associated with the ore.

DDH 4

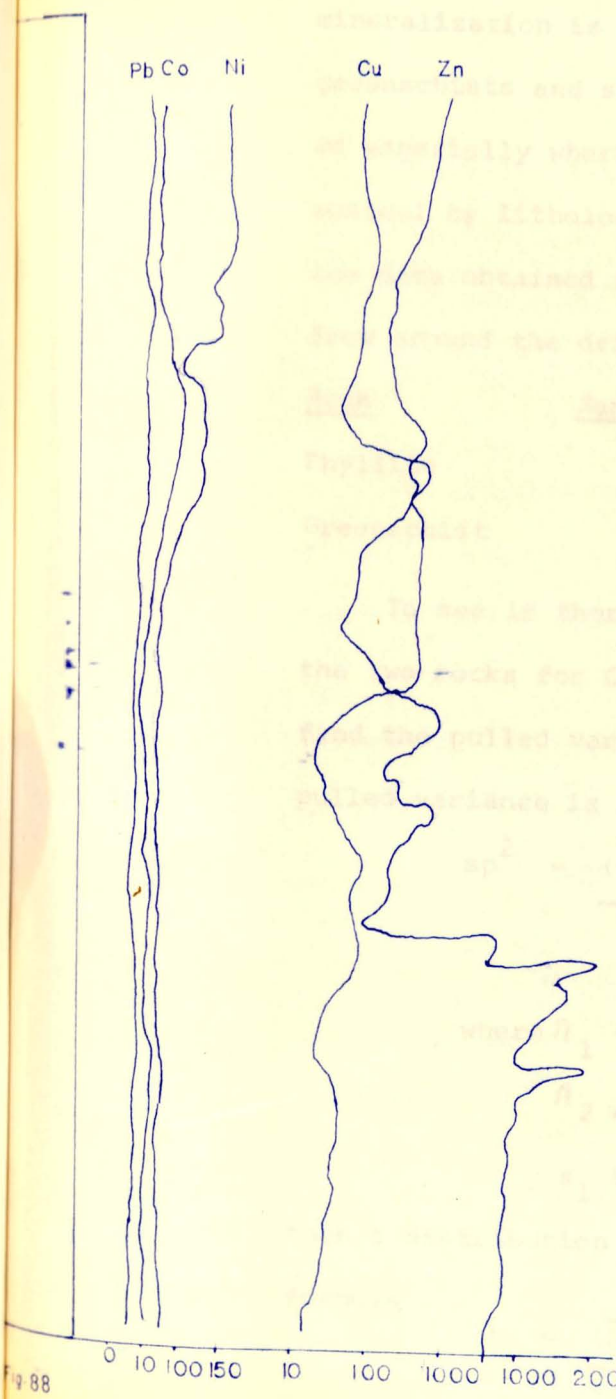

Fig 88

DDH6

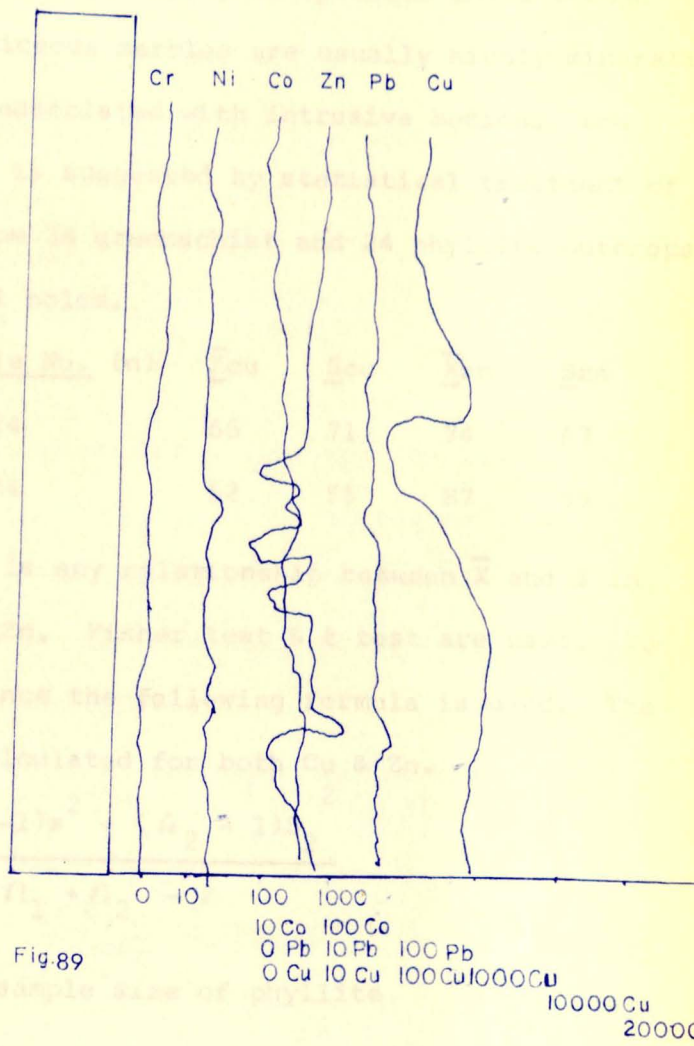

Fig 89

Vertical variation of eleme

4.3. Stratigraphic (lighologic) Relation

The copper-zinc assay data suggest that generally mineralization is not related only to specific units though greenschists and siliceous marbles are usually highly mineralized especially where associated with intrusive bodies. Low control by lithology is suggested by statistical treatment of the data obtained from 34 greenschist and 24 phyllite outcrops from around the drill holes.

Rock	Sample No. (n)	$\bar{X}$cu	Scu	$\bar{X}$zn	Szn
Phyllite	24	65	71	74	67
Greenschist	34	52	55	87	55

To see if there is any relationship between $\bar{X}$ and S in the two rocks for CuxZn. Fisher test & t test are used. To find the pulled variance the following formula is used. The pulled variance is calculated for both Cu & Zn.

$$sp^2 = \frac{(n_1 - 1)s^2 + (n_2 - 1)S_2^2}{n_1 + n_2 - 2}$$

where n_1 = sample size of phyllite

n_2 = " " " greenschist

s_1 & s_2 = stand dev. of both rocks

then t distribution test is employed using the following formula

$$t = \frac{(\bar{X}_1 - \bar{X}_2) - (N_1 - N_2)}{sp\sqrt{\frac{1}{n_1} + \frac{1}{n_2}}}$$

where $\overline{X}_1$ = mean of phyllite

$\overline{X}_2$ = " " greenschist

N_1 & N_2 populating size of phyllite &

Since N_1 is assumed to be equal to N_2 the expression $N_1 - N_2$ becomes zero.

For using the formula

$t_{cu} = 0.78$

$t_{zn} = 0.8097$

The confidence interval for t test with 5% level of significance and $k = n_1 + n_2 - 2 = 56$ degree of freedom, taken from student t criterion table is 1.96 and hence t_{cu} & t_{zn} are in the accepted range (the hypothesis that no variation between the two rocks are accepted).

Further evidence is also furnished by Fisher $F = \frac{S^2}{S^2_2}$ criteron.

$$F_{cu} = \frac{S^2_{cu\ ph}}{S^2_{cu\ sch}} = \frac{71^2}{55^2} = 1.666$$

$$F_{zn} = \frac{S^2_{zn\ ph}}{S^2_{zn\ sch}} = 67^2 = 1.484$$

The confidence interval for $F = \frac{s^2}{s^2}$ with 5% level of significance and $k = n - 1 = 23$ d.f. for phyllite & 33 d.f. for schist taken from Fisher criteron table is 1.87 since both F_{cu} & F_{zn} are below 1.87, the hypothesis that the two rocks do not differ in mineralization are accepted.

Similar calculation for other rocks show also that at least a secondary dispersion of ore forming elements is super-imposed on the primary dispersion pattern, giving rise to a scheme in which mineralization doesn't seem to be restricted to a single rock unit.

4.4. Lateral Relation (Variation)

Lateral changes in mineralization from the core samples have been studied by means of comparison of data and statistical treatment on the basis of Fisher F and student t tests. The tests are conducted on correlable greenschists in DDH_4, DDH_5, DDH_6 and DDH_7. The analytical data and the tests show that there is a decrease in mineralization from hole number DDH_4 to DDH_6; DDH_5, however, shows a higher mineralization than DDH_6 but lower than DDH_4 DDH_7 is the least of all in mineralization. Similar statistical treatment of the other rocks show the same result.

The reason for this change in mineralization is proposed to be based on the presence of intrusive bodies. Where intrusive bodies are abundant mineralization is high and vice versa.

4.5. Modal Abundance Relation

To see if any one particular type of rock forming mineral or association of minerals is related to sulphide mineralization modal analysis is done on core samples from hole number DDH_4. This modal analysis has also another importance in

showing depth variation of minerals. The data is tabulated in Table 8 and plotted in fig. 90.

The zones in which the copper assay value is 0.1% is superimposed on the modal abundance graph (fig. 91). This illustrates that the abundance of calcite in the main might be related to high copper assay value. The presence of carbonate (calcite) might have facilitated the precipitation of copper minerals from acid solutions generated from oxidation of copper and iron sulphides so giving an explanation from among the possible remobilization processes. Hence the genetic relationship of carbonates with ore minerals. On the other hand not all rocks which contain carbonate are known to be mineralized. This is seen in some cases where the two (copper ore and calcite) do not go together. Quartz carbonate veins and carbonate veins are abundant and are highly mineralized.

4.6. Tectono-metamorphic Relation

Concentrations of magnetite in pods and bands of upto 50 cms across, and dissiminated pyrite were considered to follow the deformation. Recrystallization and remobilization concentrated mineralization at depth in Katta 2, along the highly deformed interface between the plutons and the metasediments metavolcanics. The interface is characterized by the development of gneisses. Such a gneiss in the mapped area shows the highest Cu & Zn assays. Regional metamorphism also concentrated mineralization along foliation planes.

Fig. 90a Mineralogical variation with depth in DDH-4

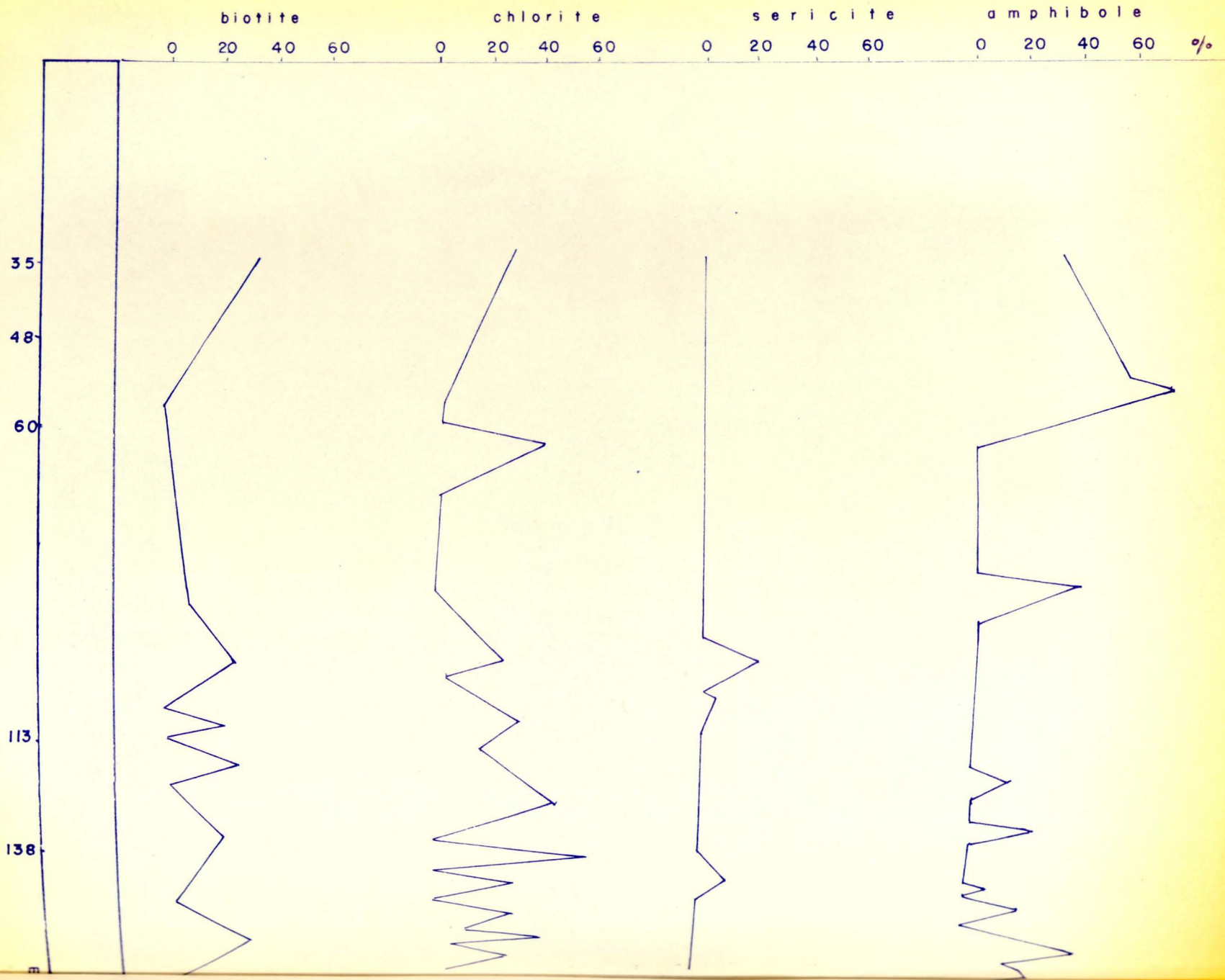

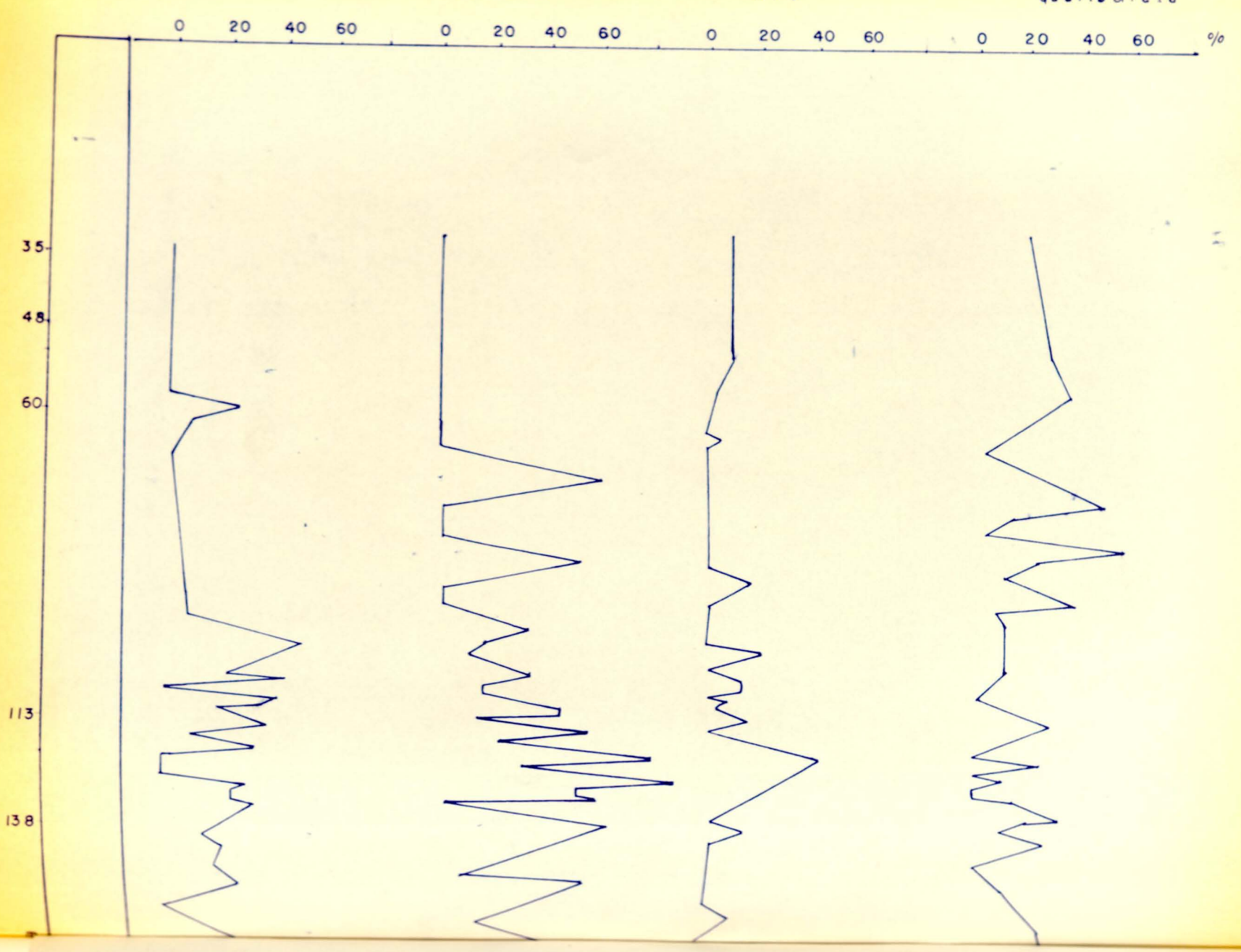
0 20 40 60
0 20 40 60
0 20 40 60
0 20 40 60
%
35
48
60
113
138

FIG. 91 high Cu value super-imposed on high Calcite % age

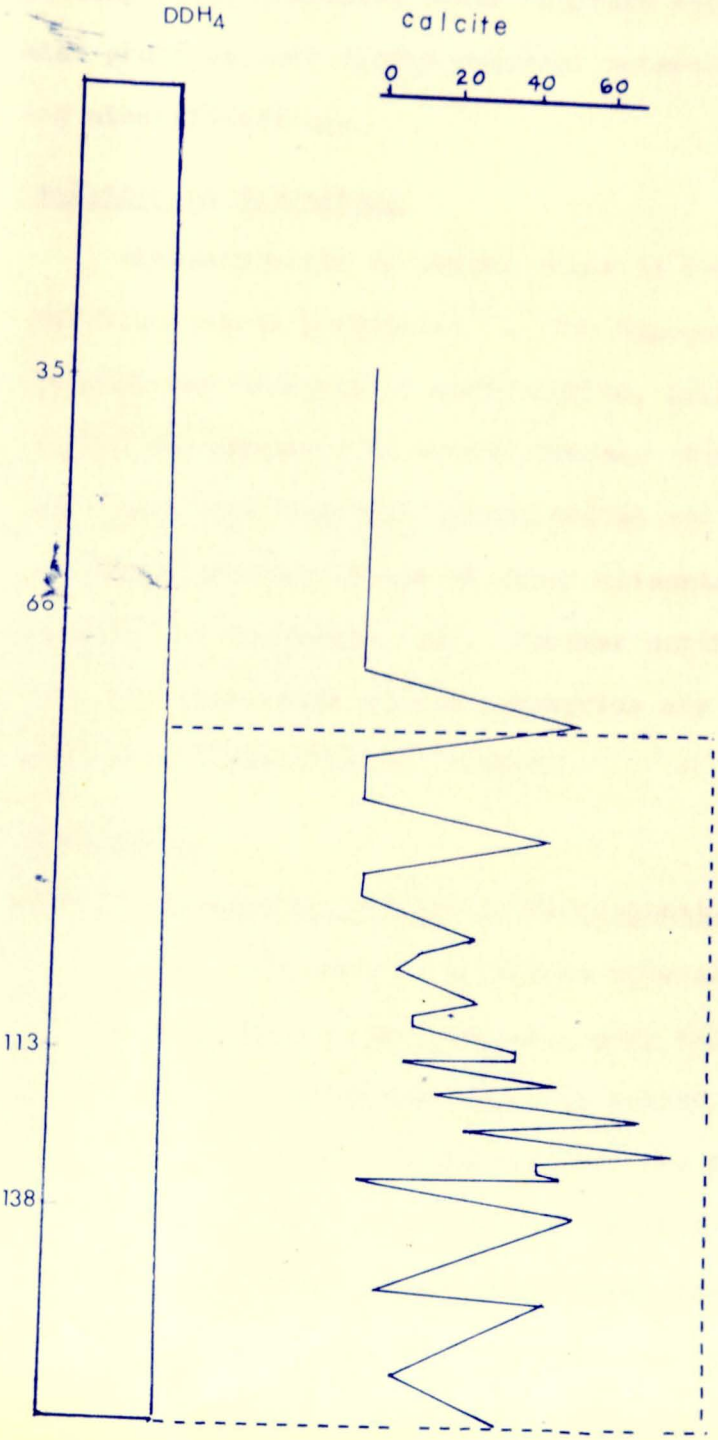

The ahomalous zone following the foliation plane and bedding plane discussed under "surface soil geochemistry" is also proof of role played regional metamorphism in concentrating mineralizations.

4.7. Relation to Intrusives

Disseminations of copper occur in some diorite intrusive and blue quartz porphyries[11]. The hypogene mineralization in diorites consists of chalcopyrite, pyrite and magnetite mostly disseminated as minute grains. The blue quartz on the other hand intruded granodiorites and metasediments and in places contain stains of minor disseminated chalcopyrite, bornite and malachite (11). Further north at Degero (see fig. 92) these blue quartz porphyries are highly mineralized (personal communication, Belay).

4.8. Ore Genesis

4.8.1. Syngenetic Stratiform Mineralization

Syngenetic stratiform mineralization occurs mainly in a conglomeratic grey coloured subunit within a sericite chlorite schist unit. Submarine volcanism is responsible for the formation of this stratiform mineralization as it is proved by the presence of metavolcanic rocks coupled with the existence of conglomerates, agglomerates and such sedimentary features as cross-bedding. The rocks in which mineralization is found was deposited in island arc environments in which much of the volcanism

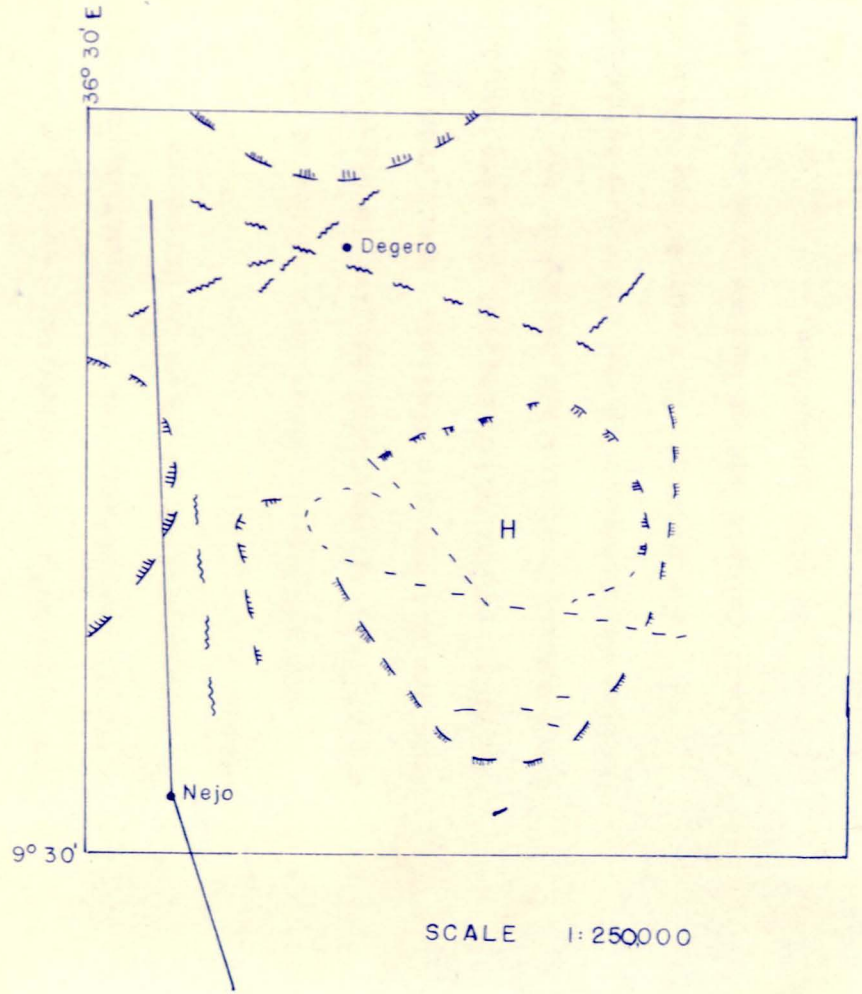

KEY

Possible Geological boundary

Possible fault

H Possible basic rock body

SURVAIR LTD. OTTAWA, CANADA

interpreted by Geoterex Ltd.

Fig. 92

SCALE 1:250000

was submarine. The submarine nature of the volcanic activity responsible for the formation of similar type of mineralization is known in different parts of the world.

The syngenetic stratiform nature of the mineralization is, as described earlier is directly concluded from ore microscopic studies. Apart from this, there are other points which suggest the same conclusion. The syngenetic stratiform nature of the deposit is further strengthened by the following evidences.

(1) The presence of about 40 cms thick barite deposit and of bedded iron stones associated with quartzites.

(2) The weight percent Pb-Zn ratios were shown in fig. 93. The ratios are characteristics of stanton's (1972)[46] stratiform sulphide ores of marine and marine-volcanic association. For comparison, stanton's data from a number of large stratiform ore deposits form Europe, North America, Africa, Australia, and the Middle East are indicated on the diagram.

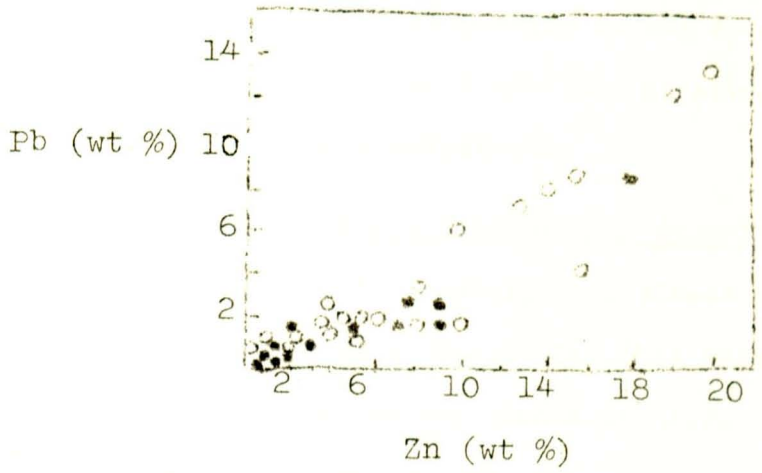

Fig. 93. Weight percent Pb-Zn ratios for Katta ores (black circle) compared with Pb-Zn ratios for Stanton's (1972) sulphide ores of marine-volcanic association.

Diagrams of the Cu-Pb-Zn ratios from the diamond drill holes examined show that the deposits fall on or near the Cu-Zn join, below a line drawn approximatel from the Cu - corner to 28% Pb on the Zn-Pb join. The data also show a tendency for the deposits to be separated into copper-rich and Zn rich types. This again is identical to Staton's discussion of stratiform sulphide ores of a marine-volcanic association on a world-wide basis. This is also confirmed by skellefte sulphide deposits in Sweden by Grip (1973)[53].

(3) The calc-alkaline submarine volcanism environment seen in most of the rocks is an added suggestion to the formation of favourable conditions for stratiform Cu-Zn-Pb mineralizations.

4.8.2. Epigenetic Vein - Disseminated Deposits

This is the main type of mineralization and the associated features with this type of mineralization in Katta are discussed here.

(1) Country Rock

The premineralization rocks in Katta are the sericite chlorite phyllite, green schists and greissose green schists intercalated with smaller and wider marble zones (1 mm to 2 m)[33]. These phyllites and schists are interpreted as fine to coarse grained metavolcaniclastics of quartz diorite composition.

(2) Intrusions

The quartz-diorite stock intruded in the previous rock series and favoured the formation of mineralization in immediately adjacent greenschists and marbles. The largest amount of mineralization can be seen in those zones with intense deformation, sometimes followed by recrystallization. From the [illegible] petrography, the fine

to medium-grained plaglocase porphyrites have a dioritic composition while the blue quartz porphyries have a more quartz dioritic composition.

(3) Veins

Calcite from the banded sedimentary marble zones has been partly remobilized by the intrusion of the quartz-diorite rocks. This is concluded from thin irregular carbonate veinlets in the green schists. In these veinlets concentrations of chalcopyrite and pyrite ore minerals are found, when the greenschists occur in the direct neighborhood of the intrusion.

(4) Alteration

a. The amphibols of the volcanics and volcanoclastics have been altered in certain zones to green biotite.

b. Followed by chlorite alteration zone.

c. The plagloclase of the porphyries have been strongly sericitized at the rim of the intrusion.

d. An epidote zone occurs in association with the carbonatized zone in and at the rim of the metavolcanic-greenschists to metavolcanoclasts. The above points are

mentioned here because of their relations to the mineralization. They are given here as colollaries to the understanding of the type of mineralization.

The Katta deposit has the following characteristics:

1. Occurrence of quartz-diorite-granodioritic intrusives - porphyries, characteristic of island arc type, associated with mineralization in country rock.
2. Presence of metavolcanoclastic country rock with carbonates.
3. Presence of alteration zones in which sericitic alteration zone is well marked in the area.
4. Vertical as well as lateral (horizontal) variation (zoning) in the elements.
5. The presence of numerous veins associated with the intrusions.
6. The low and widely distributed copper grade.
7. Its structural relationship to the plate tectonics.

Where the intrusive are incontact with intensely deformed greenschist and/or marble we find the largest amount of mineralization. (See fig. 94). The sedimentary carbonate zone, as a result of heat supplied by

LEGEND

- mineralization
- 7 sericite-talc shist
- 6 clastic sericite phillite
- 5 gneissose green shist
- 4 Marble zone
- 3 green Shist
- 2 Quartz-diorite porphyry
- 1 Quartz-Diorite intrusion

Idealized Profile showing relationship between intrusion, country rock & min.

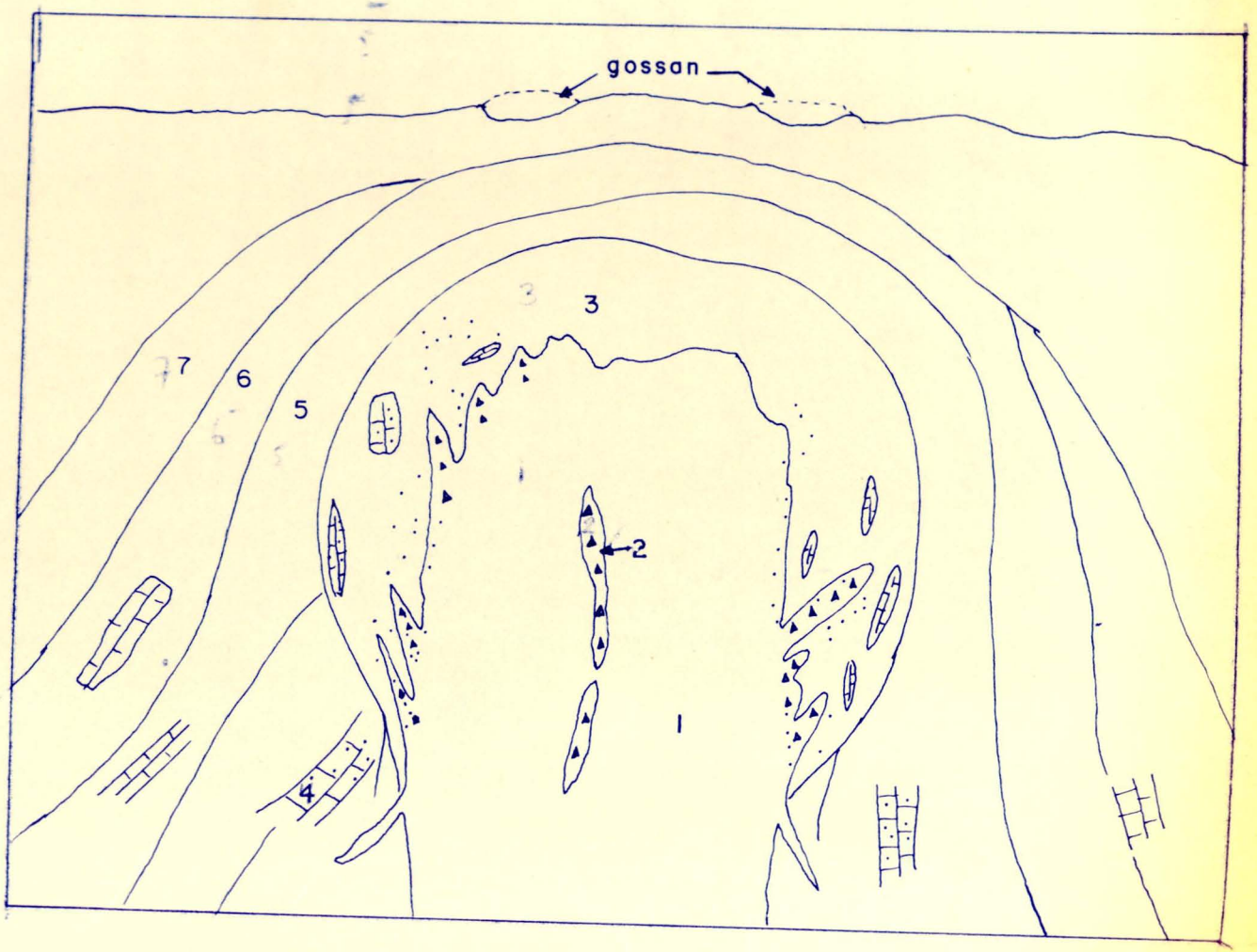

Fig. 94

the intrusives, have been remobilized and occur as veinlets of thickness ranging from 1 mm to 1 cm. The presence of these carbonates facilitates the precipitation of copper minerals from acid solutions, generated from oxidation of copper and iron sulphides. Further west, the main mineralization occurs in greenschist and in sedimentary marbles in contact with these dikes.

Coupled with the above evidences are the alteration products. The alteration was effected by the hydrothermal fluids which exchanged certain compounds with the country rocks, like addition of SiO_2 to form silica; addition of CO_2 to form carbonates; addition of Ca to form epidotes; addition of Fe to form biotite, addition of Na; K to form sericite and removal of certain compound in turn.

Characteristic vertical and lateral varation (zoning), described under "rock geochemistry and drilling", partly caused by the difference in the mobilities of the elements are established. The zoning is evidence of the participation of hydrothermal activity in the deposition of the minerals.

Geophysical surveys carried out on the area by survair limited, Ottawa, Canada and interpreted by Geoterrex Limited show huge intrusive bodies as presented in fig. 92. This may point to the possiblity of a broader extent of this type of mineralization.

4.9. Other Copper Mineralization in Ethiopia

Mineralization in the studied region is one of the many copper mineralizations which are known in Ethiopia. They are:

(1) The copper occurence controlled by blue quartz porphyry in adjacent area and further north-west about 25 kms at Degero. It was reported by de Wit et al (1978)[11]. that the blue-quartz porphyry has intruded the granodiorite and metasediments. Disseminated chalcopyrite, bornite and malachite staining have been observed in the rocks. It was also reported by the same people that this zone of blue-quartz porphyry coincides with a large geochemical copper anomaly in drill holes (upto 1300 ppm).

Float of the blue-quartz porphyry found in the hill above the granodiorite east of Katta 3 have geochemical values of upto 550 ppm.

It was felt by de Wit et al (1978)[11] that copper mineralization and the blue-quartz porphyry are magmatically related. They may extend to depth where more concentrated mineralization may occur in cementation zone.

(2) In Assosa region about 200 kms west of the mapped area exploration work is now underway.

(3) In Gojjam, a geochemical anomaly has been reported. The anomaly, however, would not normally be considered pronounced but the local copper values are higher than the adjacent areas[48].

(4) Near the border of Tigre and Beghemeder, at a place called Shiraro, copper mineralization is reported. This mineralization is thought to be associated with skarn deposits[48].

(5) In Eritrea, at a place called Tsehafi Amba disseminated type chalcopyrite, pyrite and magnetite mineralization is controlled and concentrated by a dyke like coarse feldspar porphyry intrusion. Adjacent to the porphyry the rock grades to metavolcanics such as greenschists. Mineralization is also concentrated in the metavolcanics and the calcite-chlorite veins formed as a result of the remobilization process. Further to the South in the same region, are found basic volcanics and mineralized massive metavolcancis with considerable feldspar alteration. The mineralization is mainly disseminated type. However it was also reported that mineralization often follows structures and fills cracks or occurs as veinlets. The mineralization is considered to be associated with potash feldspar alteration[48].

(6) In Debrawa, in Eritrea, the rocks belong to highly folded weakly metamorphosed sedimentary and meta-volcanics of Tsaliet group. These formations are intruded by late and post tectonic granites and other basic intrusions. Locally around Debarwa mine the series mainly composed of chlorite-quartz schist, Sericite-quartz schist and greenrocks derived from andesitic-rhyolitic rocks and volcano-genic sediments, is intruded by quartz porphyry and large basic dykes.

Mineral occurrence is of two types:

(1) Massive bedded syngenetic deposit, and

(2) Hydrothermal probably remobilized vein deposit.

Debarwa gossan outcrops is manifested by brown-ish black haematite of botryoidal habit - frequently limonitized and siliceous in parts.

Available informations say only that mineralized zone intermittently continues for about 2 kms with a maximum width of 20 meters; and consists of super-gene secondary sulphide enrichment and primary zone. The ore body extends for about 200 m with width of 51 m and about 100 m in depth. Chalcocite, bornite, alcopyrite sphalerite and pyrite and gangue minerals like quartz, barite, chlorite and sericite are found.

Examination of the structural and geological as well as mineralogical settings of all the mineralizations listed above show that they all fall in the calc-alkaline zone, discussed under general geology, which is represented by Tsaliet group in the north and Birbir group in the south. Hence these copper mineralizations may have common origin.

CHAPTER V

CONCLUSION

From the data thus obtained the most important mineralization as regards quality and quantity in Katta is the remobilized epigenetic type sulphide mineralization. This post metamorphic mineralizing process has reworked and remobilized the high background content of copper distributed throughout the rocks. The primary high copper content in the various sedimentary series is recorded by the relics of syngenetic stratabound ores related to sequences characterized by the presence of metavolcanics of submarine origin. This means that much of this mineralization (despite later metamorphic remobilization) was originally syngenetic. The metamorphic (both regional and contact) and structure related remobilization is suggested by:

(1) The presence of concentration of magnetite in pods and bands upto 50 cms across, disseminated and recrystallized pyrite in the rocks within the gneisses.

(2) The recrystallized and extensively mineralized marble in contrast to similar but barren marble away from the contact with intrusives. On a small scale throughout the area, such structurally induced mineralization of the metallic minerals and also carbonate and quartz is common, manifested by small (mm to cm) fracture, surfaces and veins filled with these materials.

The controls of the emplacement of the mineralizations are:

(a) The (hydro)(thermal) activity of the intrusives. It is

REFERENCES

1. Jelenc, D., (1966). Mineral Occurrences of Ethiopia. Addis Ababa.

2. Kent, G.R., (1970). Exploration Results on the Katta Primary Gold Occurrence (Prof. number 7): U.N. Ethiopia Mineral Survey, Wollega Province.

3. Kochemasov, G.G., (1871). Summary of Geology and Mineralization of Matti-Nejo Mineralized Belt, Wollega.

4. Metal Mining Agency of Japan (1974). Report on Geological Surv of Wollega Area, Western Ethiopia.

5. Sisay Dissasa, (1972). Geochemical Soil Sampling at Four Selec Locations in Wollega.

6. Hailu Negash, (1972). Geochemical Soil Sampling at Four Select Locations in Wollega.

7. Ahmad Mohammed and Aklilu Aseffa, (1972). Regional and Detaile Investigations on Nejo - Mendi Escarpment, Addis Ababa.

8. Fasika Mitiku, (1973). Detailed Geological Investigation of Katta Area, Minor Investigation Note 1973/4..

9. Aberra Wakjira (1973/4). Geological Investigation of Nejo Area, Minor Investigation Note 1973/3.

10. Tesfaye Lakew,(1977). Geological Report of the Katta Area, Addis Ababa University.

11. de Wit M., R. Berg, Befekadu Balcha, Alemayehu Guyasa and Teklu Bekele, (1977). A Synopsis of the Geology around Katta, Wollega with Recommendation for a Drilling Program.

12. Belay Desta, (1978). Katta Drill Hole DDK7/8, Ethiopia Institute of Geological Surveys.

13. Belay Desta, (1979). Geology of the Katta and Katta East Area. Note No. 115, Ethiopian Institute of Geological Surveys.

14. Pisarski, J., (1978). Geochemical Assessment of Western Wolleg Note No. 79. Ethiopian Institute of Geological Surveys.

15. Pisarski, J., (1978). Geological Survey of Katta Area, Wollega First Interin Report. Note No. 89. Ethiopian Institute of Geological Surveys.

16. Kazmin, V., A. Shiferaw, M. Tefera, and S. Chewaka, (1980). Metallogeny of Western Province, Ethiopia, (Unpublished Report).

17. Mohammed, Ahmad, (1980). Geochemical Overburden Exploration in Katta (unpublished Report).

18. Holmes, A., (1951). The Sequence of Precambrian Orogenic belts in South and Central Africa. Cong.Geol. International XVIIIth: London, 1948 - Report 14.

19. Cahen, and N.J. Snelling, (1966). The Geology of Equatorial Africa, Amesterdam.

20. Clifford, T.N., (1970). The Structural Framework of Africa, in "African Magmatism and Tectonics", Oliver and Bold, Edinbur

21. Dainelli, G., (1943). Geologia dell' Africa Orientale. R. Acc. Italia, Rome.

22. Beyth, M., (1971). The Geology of Central - Western Tigre.

23. Lebling, G. & E. Nowack, (1939). Geologische Forschungen in Tsehertscher Gebirge, Ost Abessiniens. Neues Yahrb. Min. 10, Beil-Bank 81.

24. Gilboy, C. and A. Chater, (1970). Stratigraphic and Structura Relations in the Shakisso-Arero Region of Southern Ethiop 14th ann.Rep.Insti.Africa. Geological University Leeds.

25. Mohr, P., (1971). Geology of Ethiopia (2nd edition) Univ. Coll. Addis Ababa Press.

26. Kazmin, V., (1971). Precambrian of Ethiopia, Nature Physici. 176-177.

27. Kazmin, V., (1971a). Geology of Ethiopia. Geological Survey Ethiopia (unpublished).

28. Kazmin, V., (1972c). Some Aspects of Precambrian Development in East Africa, Nature, Vol. 240.

29. Kazmin, V., (1972b). Granulites in Ethiopian Basement. Nature, Phys. Scienc., London, Vol. 240.

30. Kazmin, V., (1975). The Precambrian of Ethiopia and Some aspects of the Mozambique Belt, Bull. Geophys. Obs. Addis Ababa, Vol. 15.

31. Kazmin, V., (1976). Ophiolites in Ethiopian Basement. Note 35, Ethiopian Institute of Geological Surveys.

32. Kazmin, V., A. Shiferaw and T. Balcha, (1978). The Ethiopian Basement: Stratigrapju and Possible Manner of Evolution. Geological Rdsch. Vol 67.

33. S. Chewaka and M. de Wit, (1980). Plate Tectonics and Mineral Occurrence in Ethiopia.

34. Miller et al., (1967). Quoted in Kazmin, V., et al (1978). The Ethiopian Basement: Stratigraphy and possible manner of Evolution. Geol. Rdsch., Vol 67.

35. Metal Mining Agency of Japan, (1974). Report on Geological Survey of Wollega Area, Western Ethiopia (unpublished).

36. de Wit, M.J., (1977). Notes on the Geology of part of Sheet Nc - 36 - 16 (Gore). Ethiopian Institute of Geological Surveys.

37. Burk, K. and Dewey, J., (1972). Orogeny in Africa. In T.F.J. Dessauvragie and Whiteman.

38. Kroner, M.A., (1979). Pan African Plate Tectonics and its Reprecussions on the Crust of North-East Africa. Sonderd Ausder Geologischen Rundschau Band 68.

39. Spry, A., (1969). Textures of Metamorphism, Pergamon Press.

40. Turner & Verhoogen (1960). Igenous and Metamorphic Petrology, 2nd edition, McGraw-Hill Book Company, Inc.

41. Fountain, R.J., (1972). Geological Relationships in the Panfu Porphyry Copper Deposit, Bougainville Island, New Guinea. Economic Geology, Vol. 67.

42. Davis, J.C., (1973). Statistics and Data Analysis in Geology. John Wiley and Sons.

43. Koch, G.S. and Link, R.F. (1970). Statistical Analysis of Geological Data. John Wiley and Sons.

44. Soukourokov, Y., (1980). Lithochemical Prospection in Katta (unpublished).

45. Ramdohr, P., (1980). The Ore Minerals and their Intergrowths. English Translation of the 3rd edition Pergamon Press.

46. Stanton, R.L., (1972). Ore Petrology. McGraw-Hill.

47. Grip, E., (1973). Skelleftefalets sulfidmalmer, in Rickard, D.T. and Zweifel, H., (1975) Economic Geology, Vol. 70.

48. A. Mohammed (1975). Geochemical Dispersion Associated with Copper Mineralization in Ethiopia, Canada.

DECLARATION

I, the undersigned, declare that this thesis is my work and that all sources of material used for the thesis have been dully acknowledged.

Telahun Mammo

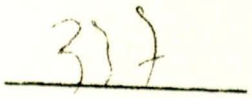

Addis Ababa, July 1980